学位論文　（要約）

Exploration of Luminescent Dipyrrin Complexes and Their Assemblies: Molecular Design, Synthesis, and Photophysics

（発光性ジピリン錯体とその集積体の探索：分子設計、合成および光物性）

平成 28 年 12 月博士（理学）申請

東京大学大学院理学系研究科

化学専攻

土屋　瑞穂

Abstract

In this thesis, I focus on new series of luminescent dipyrrinato complexes. Here, I designed dipyrrinato complexes showing fluorescence in solution and aggregate states and achieved their synthesis and analysis of their properties, mainly their photophysical properties. The contents of each chapter are described in detail below.

In Chapter 1, general introduction of fluorescent molecules and dipyrrins is made. The importance, versatility, applications of fluorescent molecules are explained first, then dipyrrins, excellent candidates for such molecules, are introduced.

In Chapter 2, solid-state luminescence of bis(dipyrrinato)zinc(II) complexes is revealed. The design, synthesis, and analysis of their photophysics are achieved.

In Chapter 3, imine-linked BODIPY oligomers are developed and their photophysical, electrochemical, and thermogravimetric properties are revealed. The versatility of imine-linked BODIPY is demonstrated, with intense and tunable fluorescence.

In Chapter 4, concluding remarks of this thesis are described.

Contents

Chapter 1

Introduction

1.1 Photofunctional molecules

Photofunctional molecules – molecules interact with light to give a certain output – have been a major field of chemistry, fascinating synthetic and materials chemists, in view of utilizing light as energy source, signals, etc. In photofunctional molecules, absorbed light goes through the molecules to result in an output. Note that such molecules can contain multiple photofunctional subunits, which can cooperate to achieve certain functionalities (Figure 1.1.1). Developed functionalities include artificial light-harvesting[1-3], photo-catalysis[4,5], photo-sensitizing[6], upconversion[7,8], photo-switching[9-11], etc. Numerous types of structures have been developed thus far, attempting to achieve and improve such functionalities. Although some of them are utilized as devices such as organic light-emitting diodes (OLEDs)[12-14] and dye-sensitized solar cells (DSSCs)[15-17], the other ones are still confined to basic development. To improve their functionalities, further knowledge and insight into the synthesis and photophysical and photochemical properties of photofunctional molecules are in demand.

In this thesis, of the diverse fields of photofunctional materials, photoluminescent materials, especially fluorescent materials, are the point of focus. Fluorescence has long been of great interest, and numerous molecules have been developed not only for scientific interest, but applications as luminescent devices[13,14], fluorescent dyes[18-20], bioimaging markers[21-25], and molecular machines[26]. For some of such applications, it is often mandatory to assemble multiple fluorescent structures to attain the desired functionalities. In such assemblies, the number, orientation, and distance between the fluorescent structures play key roles in determining the type and intensity of the interactions, affecting the functionalities of the resultant assemblies. Development of fluorescent structures and methods to link the structures in designated distance, orientation, etc, and insight into such assemblies would contribute to the field of photoluminescent materials. The next sections portray dipyrrins and their complexes, versatile photoluminescent materials.

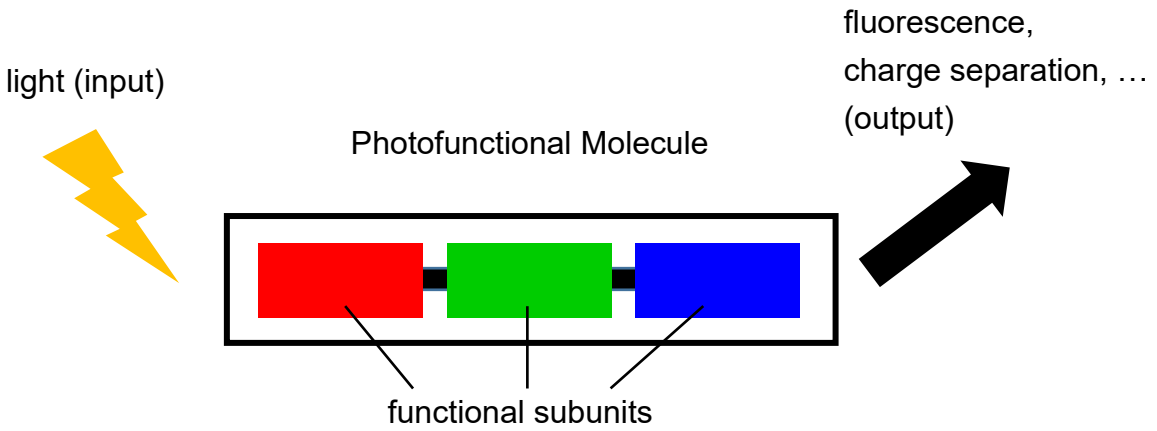

Figure 1.1.1. The concept of a photofunctional molecule. Input light is absorbed into the photofunctional molecule with one or more functional subunits, returning an output.

1.2 Dipyrrins and their complexes

1.2.1 Dipyrrins and their metal complexes

Dipyrrins, or dipyrromethenes, are a class of organic molecules whose structures are characterized by two pyrrolic rings attached with a methine bridge at their α-positions (Figure 1.2.1.1)[27]. They are known for intense absorption in the visible region (molar extinction coefficients (ε) ~ 10^5 $M^{-1}cm^{-1}$ and absorption wavelength (λ_{abs}) ~ 500 nm), derived from the $^1\pi$-π^* transition. The intense absorption render them as desirable chromophores, or light absorbents. In addition, thanks to their two pyrrolic nitrogen atoms, they can serve as monovalent, bidentate ligands, allowing them to coordinate to various cationic species. Overall, dipyrrins can serve as both chromophores and ligands. They are also featured by chemical and photochemical stability, rendering themselves as building blocks for photofunctional systems. Since there are numerous chemical modification methods known, their physical, chemical, spectroscopic, and other properties can be tuned by introducing certain functional groups; they can serve as versatile photofunctional materials.

As described above, dipyrrins can coordinate to various cations to form complexes. Thus far, numerous metal complexes have been reported; the cationic species include Fe(III), Co(II) , Ni(II), Cu(I), Zn(II), Ga(III), In(III) [27-32], etc in the forms of mono-, bis-, and tris- complexes. For bis- and tris(dipyrrinato) metal complexes, since multiple dipyrrin ligands coordinate the metal center, supramolecules and coordination polymers have been developed, utilized as metal organic frameworks (MOFs)[33-36], energy transfer systems[37], charge separation systems[38], etc (Figure 1.2.1.2). These examples utilize dipyrrins as both the linkage and chromophoric moieties.

Although dipyrrins' transition metal complexes do not emit fluorescence because of non-fluorescent d-d transition, some of them, without such transition, are known to exhibit intense fluorescence; dipyrrinato complexes with Zn(II), Cu(I), Cd(II), Ga(III), and In(III), metal ions without a vacant d orbital, are known to show fluorescence depending of the type of the linker moiety[28-29]. Of those, zinc complexes are known as the most fluorescent complexes.

Along with the metal ions above, other types of cations can accept dipyrrin ligands. Such cationic species include SiR_2^{2+} [39] and BR_2^{+} [40-43] (the R stands for a functional group). They are both known to be fluorescent, and the latter complexes are often abbreviated as BODIPYs. BODIPYs are the most famous dipyrrins' complexes, often utilized as fluorescent and laser dyes, tags, and numerous other purposes owing to their intense fluorescence.

In summary, dipyrrins and their complexes are versatile materials, especially in terms of photofunctionalities. The next sections describe bis(dipyrrinato)zinc(II) complexes and BODIPYs, the most fluorescent and promising dipyrrinato complexes.

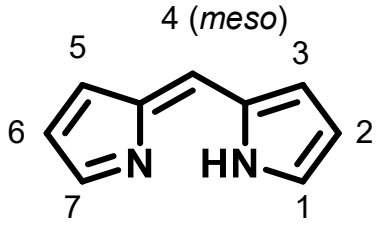

Figure 1.2.1.1. The structure of a dipyrrin. The numbers represent the positions.

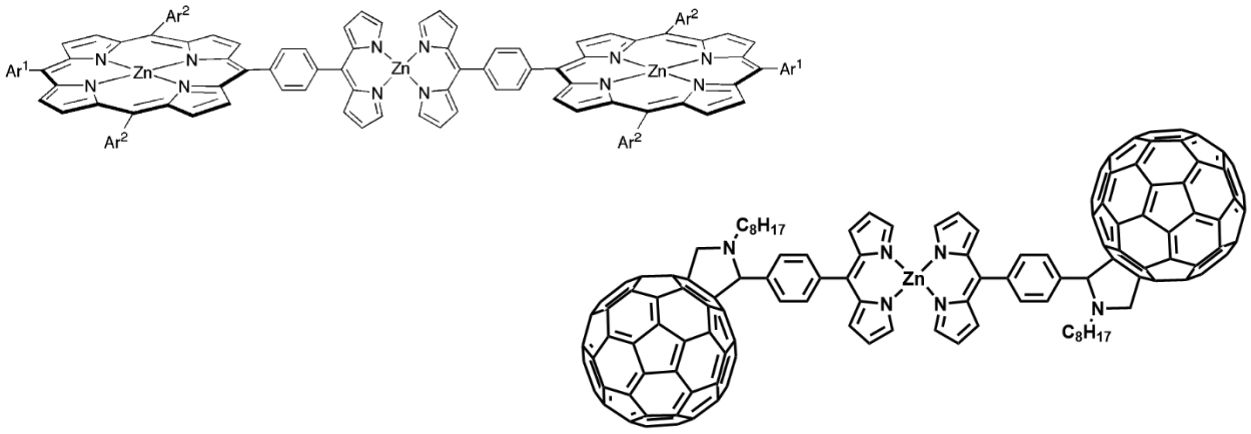

Figure 1.2.1.2. A charge separation system[37] (left) and an energy transfer system[38] (right) based on a bis(dipyrrinato)zinc(II) complex subunit. Adapted with permission from ref. 37. Copyright 2003 American Chemical Society (top).

1.2.2 Bis(dipyrrinato)zinc(II) complexes

As described in Section 1.2.1, bis(dipyrrinato)zinc(II) complexes are known to be fluorescent. Although they had been known as weakly luminescent complexes before the work by Lindsey[44], who has attributed the cause of quenching to the rotation of the *meso*-aryl rings, which provides non-radiative decay channels (Figure 1.2.2.1). They prepared a bis(dipyrrinato)zinc(II) complex with a bulky mesityl group at the *meso* position to eliminate the decay pathways by the rotational modes, which fluoresces with ϕ_F of 0.36 in toluene – a 60-fold enhancement of fluorescence from a *meso*-phenyl complex – showing the efficacy of placing a bulky group on the *meso*-position. Our group has found a way to improve the luminescence quantum yields of bis(dipyrrinato)zinc(II) complexes by applying a different strategy. Designing bis(dipyrrinato)zinc(II) complexes heteroleptic, the fluorescence quantum yields drastically improved to 0.79 (toluene) in solution[45,46] (Figure 1.2.2.2).

Since bis(dipyrrinato)zinc(II) complexes afford the construction of supramolecules and coordination polymers, such molecules have also been developed. During my master course, I have developed energy transfer systems comprised of heteroleptic bis(dipyrrinato)zinc(II) complexes showing quantitative energy transfer[46]. Maeda et al. developed luminescent coordination polymer aggregates and a polygon-like structure showing conductivity[47].

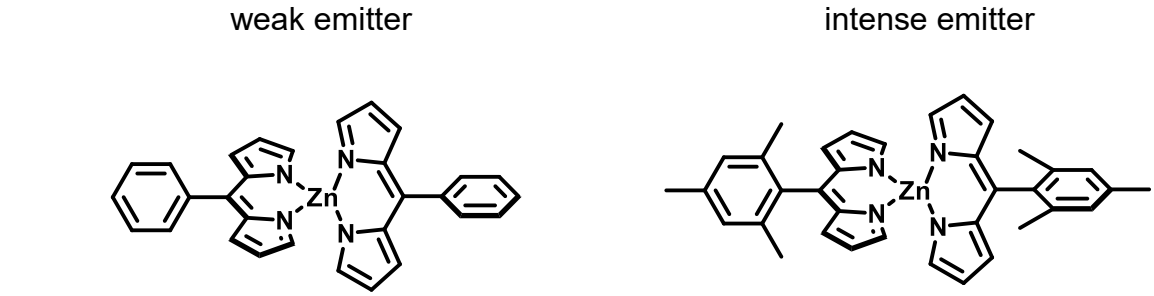

Figure 1.2.2.1. Bis(dipyrrinato)zinc(II) complexes with *meso*-phenyl (left) or -mesityl groups. The former shows a fluorescence quantum yield (ϕ_F) of 0.006 in toluene, while the latter emits with an improved ϕ_F of 0.36 in toluene[44].

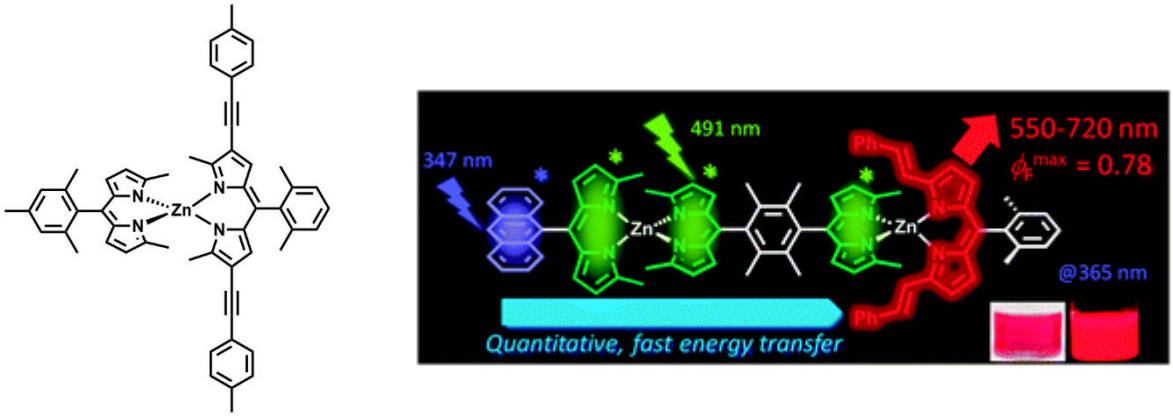

Figure 1.2.2.2. A luminescent heteroleptic complex (left)[45] and an asymmetric heteroleptic bis(dipyrrinato)zinc(II) complex (right)[46]. Reproduced from ref. 46 with permission from the Royal Society of Chemistry (right).

1.2.3 BODIPYs (boron-dipyrromethenes)

Dipyrrins' boron complexes, BODIPYs, are the most famous series of dipyrrinato complexes. They are a class of organic molecules bearing a disubstituted boron cation, the most common species being BF_2^+. They are known to show intense fluorescence often reaching a fluorescence quantum yield close to unity even in polar solvents, such as methanol. In addition, BODIPYs inherit all the favorable properties of dipyrrins such as intense absorption, stability, and the availability of chemical modification methods, rendering themselves as excellent chromophores and fluorophores.[40-43]

To date, a vast number of reports have been published regarding BODIPYs, from fundamental to applied sciences. Many BODIPYs have been developed, showing different absorption and emission wavelengths, Stokes shift, molecular levels, sensitivity to the environment, etc. BODIPYs are also utilized as fluorescent dyes, probes, laser dyes, photo-sensitizers, etc.[6,40-43,48], In fundamental sciences, using multiple BODIPYs as photofunctional modules, systems achieving certain functionalities are reported. For example, Ziessel et al. have achieved energy funneling systems, collecting photo-excited energy from the peripheral to the center (Figure 1.2.3.2)[49-51]. Another example utilizes BODIPYs as photosensitizers, conveying energy from one side to the other side, which is passed to the singlet generating BODIPY subunit (Figure 1.2.3.3)[52,53]. Multiple BODIPYs afford energy absorption, mediation, and emission, which cooperate to result in certain functionalities.

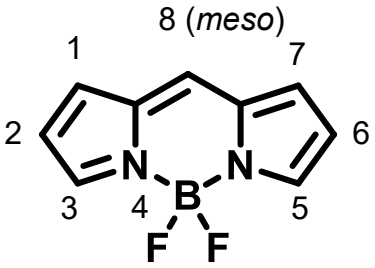

Figure 1.2.3.1. The structure of BODIPY.

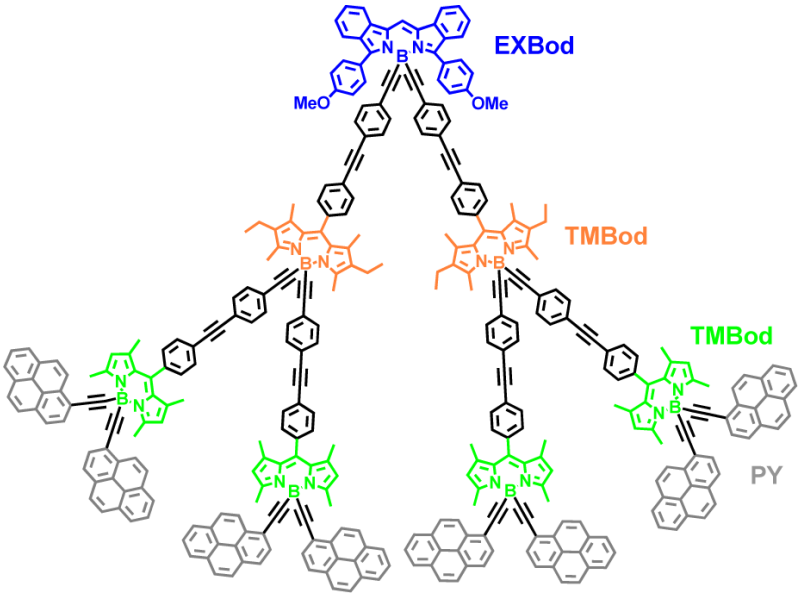

Figure 1.2.3.2. An artificial light-harvesting system by stepwise energy transfer from the peripheral to the center.[49] Adapted with permission from ref. 49. Copyright 2013 American Chemical Society.

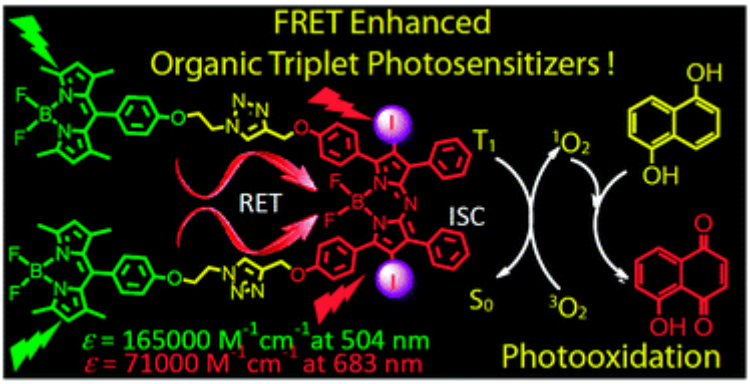

Figure 1.2.3.3. A BODIPY-based photosensitizer, using BODIPY subunits as the absorbents and sensitizers.[53] Reproduced from ref. 53 with permission from the Royal Society of Chemistry.

1.3 Aim of this study

So far, applications and the importance of photofunctional molecules have been described. Dipyrrins and their complexes were mentioned as promising and versatile chromophores. In this study, exploration of luminescent dipyrrinato complexes was conducted. Molecular design of fluorescent dipyrrinato complexes is devised throughout the study, focusing on the distance and orientation of dipyrrin cores. Since spacing or bridging units joining dipyrrin cores affect the distance, orientation, and electronic communication between the dipyrrin cores, the study focused on the design and role of bridging units. The synthesis and analysis on their photophysical properties are conducted. Here, the chemistry of dipyrrins is explored, and new series of luminescent dipyrrinato metal complexes and their assemblies are developed.

1.4 References

1. Aratani, N.; Kim, D.; Osuka, A. *Acc. Chem. Res.* **2009**, *42*, 1922–1934.
2. Jeong, Y. H.; Son, M.; Yoon, H.; Kim, P.; Lee, D. H.; Kim, D.; Jang, W. D. *Angew. Chem. Int. Ed.* **2014**, *53*, 6925–6928.
3. Balaban, T. S. *Acc. Chem. Res.* **2005**, *38*, 612–623.
4. Lin, X. H.; Lee, S. N.; Zhang, W.; Li, S. F. Y. *J. Hazard. Mater.* **2016**, *303*, 64–75.
5. Irmler, P.; Winter, R. F. *Dalton Trans.* **2016**, *45*, 10420–10434.
6. Kamkaew, A.; Lim, S. H.; Lee, H. B.; Kiew, L. V.; Chung, L. Y.; Burgess, K. *Chem. Soc. Rev.* **2013**, *42*, 77–88.
7. Singh-Rachford, T. N.; Castellano, F. N. *Coord. Chem. Rev.* **2010**, *254*, 2560–2573.
8. Monguzzi, A.; Tubino, R.; Hoseinkhani, S.; Campione, M.; Meinardi, F. *Phys. Chem. Chem. Phys.* **2012**, *14*, 4322–4332.
9. Yun, C.; You, J.; Kim, J.; Huh, J.; Kim, E. *J. Photochem. Photobiol. C Photochem. Rev.* **2009**, *10*, 111–129.
10. Irie, M. *Chem. Rev.* **2000**, *100*, 1685–1716.
11. Fukaminato, T.; Doi, T.; Tamaoki, N.; Okuno, K.; Ishibashi, Y.; Miyasaka, H.; Irie, M. *J. Am. Chem. Soc.* **2011**, *133*, 4984–4990.
12. Sasabe, H.; Kido, J. *Eur. J. Org. Chem.* **2013**, No. 34, 7653–7663.
13. Sasabe, H.; Kido, J. *J. Mater. Chem. C* **2013**, *1*, 1699–1707.
14. Kido, J.; Kimura, M.; Nagai, K. *Science* **1995**, *267*, 1332–1334.
15. Grätzel, M. *J. Photochem. Photobiol. C Photochem. Rev.* **2003**, *4*, 145–153.
16. Hagfeldt, A.; Boschloo, G.; Sun, L.; Kloo, L.; Pettersson, H. *Chem. Rev.* **2010**, *110*, 6595–6663.
17. Gong, J.; Sumathy, K.; Qiao, Q.; Zhou, Z. *Renew. Sustainable Energy Rev.* **2017**, *68*, 234–246.

18. Fei, X.; Gu, Y. *Prog. Nat. Sci.* **2009**, *19*, 1–7.

19. Breul, A. M.; Hager, M. D.; Schubert, U. S. *Chem. Soc. Rev.* **2013**, *42*, 5366–5407.

20. Dsouza, R. N.; Pischel, U.; Nau, W. M. *Chem. Rev.* **2011**, *111*, 7941–7980.

21. Zhang, J.; Campbell, R. E.; Ting, A. Y.; Tsien, R. *Nat. Rev. Mol. Cell Biol.* **2002**, *3*, 906–918.

22. Fernandez-Suarez, M.; Ting, A. Y. *Nat. Rev. Mol. Cell Biol.* **2008**, *9*, 929–943.

23. Chan, J.; Dodani, S. C.; Chang, C. J. *Nat. Chem.* **2012**, *4*, 973–984.

24. Kim, J. S.; Quang, D. T. *Chem. Rev.* **2007**, *107*, 3780–3799.

25. Johnson, I. *Histochem. J.* **1998**, *30*, 123–140.

26. André, J.; Pischel, U. *Chem. Soc. Rev.* **2015**, *44*, 1053–1069.

27. Wood, T. E.; Thompson, A. *Chem. Rev.* **2007**, *107*, 1831–1861.

28. Sakamoto, R.; Iwashima, T.; Tsuchiya, M.; Toyoda, R.; Matsuoka, R.; Kögel, J. F.; Kusaka, S.; Hoshiko, K.; Yagi, T.; Nagayama, T.; Nishihara, H. *J. Mater. Chem. A* **2015**, *3*, 15357–15371.

29. Baudron, S. A. *Dalton Trans.* **2013**, *42*, 7498–7509.

30. Ding, Y.; Tang, Y.; Zhu, W.; Xie, Y. *Chem. Soc. Rev.* **2015**, *44*, 1101–1112.

31. Cohen, S. M.; Halper, S. R. *Inorganica Chim. Acta* **2002**, *341*, 12–16.

32. Thoi, V. S.; Stork, J. R.; Magde, D.; Cohen, S. M. *Inorg. Chem.* **2006**, *45*, 10688–10697.

33. Halper, S. R.; Do, L.; Stork, J. R.; Cohen, S. M.*J. Am. Chem. Soc.* **2006**, *128*, 15255–15268.

34. Halper, S. R.; Cohen, S. M. *Inorg. Chem.* **2005**, *44*, 486–488.

35. Béziau, A.; Baudron, S. A.; Fluck, A.; Hosseini, M. W. *Inorg. Chem.* **2013**, *52*, 14439–14448.

36. Béziau, A.; Baudron, S. A.; Guenet, A.; Hosseini, M. W. *Chem. Eur. J.* **2013**, *19*, 3215–3223.

37. Yu, L.; Muthukumaran, K.; Sazanovich, I. V; Kirmaier, C.; Hindin, E.; Diers, J. R.; Boyle, P. D.; Bocian, D. F.; Holten, D.; Lindsey, J. S. *Inorg. Chem.* **2003**, *42*, 6629–6647.

38. Rio, Y.; Sánchez-García, D.; Seitz, W.; Torres, T.; Sessler, J. L.; Guldi, D. M. *Chem. Eur. J.* **2009**, *15*, 3956–3959.

39. Sakamoto, N.; Ikeda, C.; Yamamura, M.; Nabeshima, T. *J. Am. Chem. Soc.* **2011**, *133*, 4726–4729.

40. Loudet, A.; Burgess, K. *Chem. Rev.* **2007**, *107*, 4891–4932.

41. Ulrich, G.; Ziessel, R.; Harriman, A. *Angew. Chem. Int. Ed.* **2008**, *47*, 1184–1201.

42. Ziessel, R.; Ulrich, G.; Harriman, A. *New J. Chem.* **2007**, *31*, 496–501.

43. Benniston, A. C.; Copley, G. *Phys. Chem. Chem. Phys.* **2009**, *11*, 4124–4131.

44. Sazanovich, I. V.; Kirmaier, C.; Hindin, E.; Yu, L.; Bocian, D. F.; Lindsey, J. S.; Holten, D. *J. Am. Chem. Soc.* **2004**, *126*, 2664–2665.

45. Kusaka, S.; Sakamoto, R.; Kitagawa, Y.; Okumura, M.; Nishihara, H. *Chem. Asian J.* **2012**, *7*, 907–910.

46. Tsuchiya, M.; Sakamoto, R.; Kusaka, S.; Kitagawa, Y.; Okumura, M.; Nishihara, H. *Chem. Commun.* **2014**, *50*, 5881 –5883.

47. Maeda, H.; Akuta, R.; Bando, Y.; Takaishi, K.; Uchiyama, M.; Muranaka, A.; Tohnai, N.; Seki, S. *Chem. Eur. J.* **2013**, *19*, 11676–11685.

48. Awuah, S. G.; You, Y. *RSC Adv.* **2012**, *2*, 11169–11183.

49. Ziessel, R.; Ulrich, G.; Haefele, A.; Harriman, A. *J. Am. Chem. Soc.* **2013**, *135*, 11330–11344.

50. Iehl, J.; Nierengarten, J. F.; Harriman, A.; Bura, T.; Ziessel, R. *J. Am. Chem. Soc.* **2012**, *134*, 988–998.

51. Ziessel, R.; Harriman, A. *Chem. Commun.* **2011**, *47*, 611–631.

52. Huang, L.; Cui, X.; Therrien, B.; Zhao, J. *Chem. Eur. J.* **2013**, *19*, 17472–17482.

53. Guo, S.; Ma, L.; Zhao, J.; Küçüköz, B.; Karatay, A.; Hayvali, M.; Yaglioglu, H. G.; Elmali, A. *Chem. Sci.* **2014**, *5*, 489–500.

Chapter 2

Solid-state luminescence of bis(dipyrrinato)zinc(II) complexes

2.1 Introduction

To date, fluorescent materials have contributed in technology and science in many respects, such as artificial light-harvesting[1-3], photo-catalysis[4,5], and organic light emitting diodes[6-8]. Bis(dipyrrinato)zinc(II) complexes have attracted much attention as photofunctional materials, owing to their intense absorption and emission, availability of various chemical modification methods, and chemical and photochemical stability[9-14]. Although their fluorescence has been studied to a certain extent, reports had been confined to fluorescence in solution; there had hardly been any report on the fluorescence of bis(dipyrrinato)zinc(II) complexes in the solid state[15], which can find potential applications as light-harvesting and light-emitting devices.

Although there is only one report on studying solid-state fluorescence of bis(dipyrrinato)zinc(II) complexes, BODIPYs, their analogous complexes, are known to emit in the solid state under certain molecular designs. Akkaya et al. reported that by introducing bulky functional groups onto the *meso*-position of BODIPYs, the fluorescence of the BODIPYs enhanced because of more spacious packing structures, reducing the effect of aggregation caused quenching (ACQ), induced by proximity of fluorophore moieties[16]. Introduction of bulky functional groups to fluorophores is an effective method in enhancing the fluorescence properties of fluorophores.

In this research, the fluorescence properties of bis(dipyrrinato)zinc(II) complexes with different *meso*-aryl groups were studied, disclosing the fluorescence properties of the complexes in the solid state. Their fluorescence was discussed in relation to their crystal structures.

2.2 Experimental

2.2.1 Materials

1aH, **1cH**, **1a$_2$Zn**, and **1c$_2$Zn** were synthesized according to a previous report.[13] All chemicals were purchased from Tokyo Chemical Industry Co., Ltd., Kanto Chemical Co., or Wako Pure Chemical Industries, Ltd. and used without further purification. The rest of the materials were newly obtained according to Scheme 2.2.1.

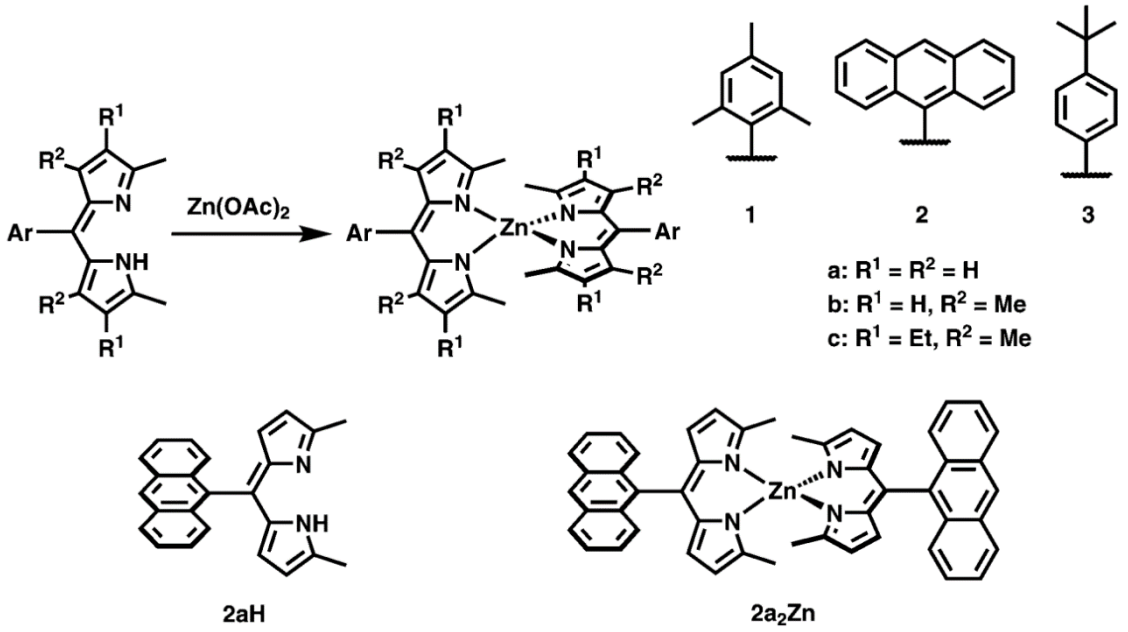

Scheme 2.2.1. Synthesis of dipyrrin ligands and bis(dipyrrinato)zinc(II) complexes.

2.2.2 Dipyrrin Ligand 2aH

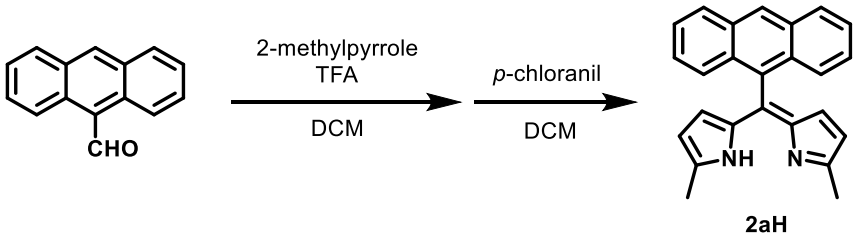

To a dichloromethane solution (20 mL) of 9-anthracenecarboxaldehyde (0.501 g, 2.4 mmol) and 2-methylpyrrole (0.43 mL, 5.0 mmol), was added trifluoroacetic acid (10 μL, 0.13 mmol) and stirred overnight at room temperature. *p*-Chloranil (0.603 g, 2.4 mmol) was added and stirred another 2 h. The reaction mixture was processed by column chromatography (alumina, dichloromethane) and recrystallization (methanol/dichloromethane) to give the pure product. Yield: 0.407 g (48 %), brown powder. ^{1}H NMR (500 MHz, $CDCl_3$): δ = 8.52 (s, 1H), 8.02 (d, J = 8.6 Hz, 2H), 7.92 (d, J = 8.6 Hz, 2H), 7.43 (t, J = 7.8 Hz, 2H), 7.34 (t, J = 7.8 Hz, 2H), 5.99 (d, J = 4.2 Hz, 2H), 5.87 (d, J = 4.2 Hz, 2H), 2.48 (s, 6H); ^{13}C NMR (125 MHz, $CDCl_3$): δ =153.85, 141.14, 134.49, 131.14, 131.11, 130.88, 128.59, 128.09, 127.36, 126.87, 125.80, 125.15, 117.89, 16.38; HR-FAB-MS: 349.1687 $[M+H]^+$, calcd. for: $C_{25}H_{21}N_2^+$: 349.1699.

2.2.3 Bis(dipyrrinato)zinc(II) Complex $2a_2Zn$

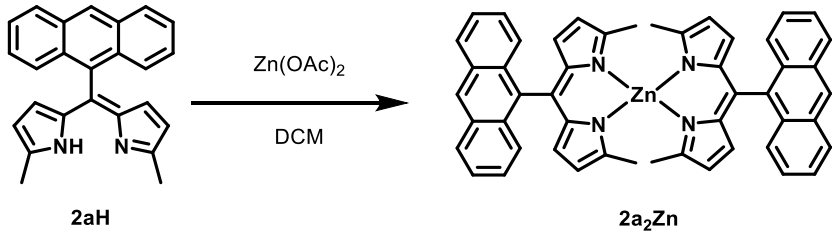

2aH **$2a_2Zn$**

To a dichloromethane solution (10 mL) of **2aH** (0.18 g, 0.50 mmol), was added a methanol (20 mL) solution of zinc acetate (48 mg, 0.25 mmol). After stirring overnight, the amount of the solvent was reduced by a rotary evaporator. The brown precipitate was collected and rinsed thoroughly with methanol. Yield: 0.183 g (96%), brown powder. ^{1}H NMR (500 MHz, $CDCl_3$): δ = 8.58 (s, 2H), 8.07 (d, J = 8.5 Hz, 4H), 8.00 (d, J = 8.8 Hz, 4H), 7.49-7.46 (m, 4H), 7.41-7.37 (m, 4H), 6.12 (s, 8H), 2.41 (s, 12H); ^{13}C NMR (125 MHz, $CDCl_3$): δ=159.14, 141.04, 140.29, 133.12, 132.93, 131.44, 130.91, 128.15, 127.25, 127.02, 125.85, 125.13, 117.67, 16.81; HR-ESI-MS: 1539.4674 $[2M+Na]^+$, calcd. for: $(C_{50}H_{38}N_4Zn)_2Na^+$: 1539.4646.

2.2.4 Dipyrrin Ligand 2bH

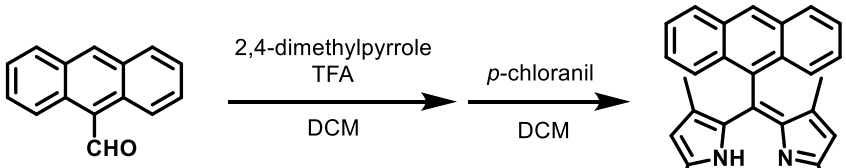

2bH

To a dichloromethane solution (30 mL) of 9-anthracenecarboxaldehyde (2.06 g, 10.0 mmol), were added 2,4-dimethylpyrrole (2.25 mL, 23.0 mmol) and trifluoroacetic acid (30 μL, 0.39 mmol). After stirring overnight, *p*-chloranil (2.45 g, 10.0 mmol) was added to the solution and stirred for 20 min. The solvent was evaporated and the residue was purified by alumina column chromatography (hexane: dichloromethane = 2:1). The orange-brown band was collected and evaporated to give the product. Yield: 0.910 g (24 %), yellow powder. ^{1}H NMR (500 MHz, $CDCl_3$): δ = 8.52 (s, 1H), 7.99 (t, J = 7.5 Hz, 4H), 7.46-7.43 (m, 2H), 7.38-7.35 (m, 2H), 5.76 (s, 2H), 2.41 (s, 6H), 0.51 (s, 6H); ^{13}C NMR (125 MHz, $CDCl_3$): δ=151.69, 140.08, 137.41, 134.97, 131.87, 131.42, 130.60, 128.16, 127.30,

126.25, 125.88, 125.42, 119.44, 16.19, 13.57; HR-FAB-MS: 377.2011 $[M+H]^+$, calcd. for: $C_{27}H_{25}N_2^+$: 377.2018.

2.2.5 Bis(dipyrrinato)zinc(II) Complex $2b_2Zn$

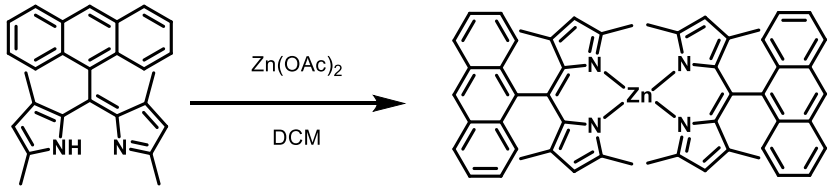

2bH **$2b_2Zn$**

To a dichloromethane solution (10 mL) of **2bH** (0.116 g, 0.500 mmol), was added a methanol (20 mL) solution of zinc acetate (0.048 g, 0.26 mmol). After stirring overnight, the amount of the solvent was reduced by a rotary evaporator. The brown precipitate was collected and rinsed thoroughly with methanol. Yield: 0.110 g (100%), brown powder. ^{1}H NMR (500 MHz, $CDCl_3$): δ = 8.56 (s, 2H), 8.06 (t, J = 8.5 Hz, 8H), 7.48-7.45 (m, 4H), 7.40-7.36 (m, 4H), 5.89 (s, 4H), 2.33 (s, 12H), 0.48 (s, 12H); ^{13}C NMR (125 MHz, $CDCl_3$): δ =156.81, 143.92, 140.82, 136.56, 134.08, 131.65, 130.93, 128.16, 127.23, 126.31, 125.66, 125.40, 120.35, 16.60, 14.97; HR-ESI-MS: 1651.5920 $[2M+Na]^+$, calcd. for: $(C_{54}H_{46}N_4Zn)_2Na^+$: 1651.5925.

2.2.6 Dipyrrin Ligand 2cH

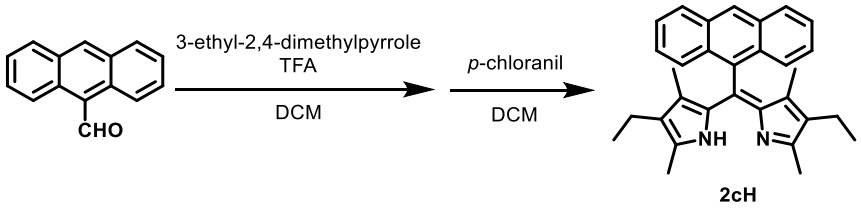

2cH

To a dichloromethane solution (50 mL) of 9-anthracenecarboxaldehyde (1.03 g, 5.00 mmol), were added 3-ethyl-2,4-dimethylpyrrole (1.05 mL, 11.3 mmol) and trifluoroacetic acid (50 μL, 0.65 mmol). After stirring overnight, *p*-chloranil (1.23 g, 5.00 mmol) was added to the solution and stirred for 20 min. The solvent was evaporated and the residue was purified by alumina column chromatography (hexane: dichloromethane = 2:1). Yield: 0.642 g (30 %), brown powder. ^{1}H NMR (500 MHz, $CDCl_3$):

δ = 8.52 (s, 1H), 8.02-7.99 (m, 4H), 7.45-7.42 (m, 2H), 7.37-7.33 (m, 2H), 2.38 (s, 6H) , 2.14 (q, J = 7.6 Hz, 4H) , 2.48 (t, J = 7.6 Hz, 6H) , 0.40 (s, 6H) pyrrolic proton signal (1H) missing due to broadening; ^{13}C NMR (125 MHz, $CDCl_3$): δ=150.20, 137.03, 134.44, 133.38, 132.78, 131.40, 131.03, 130.80, 128.06, 127.04, 126.24, 125.98, 125.33, 17.48, 14.83, 14.55, 10.66; HR-FAB-MS: 432.2648 $[M+H]^+$, calcd. for: $C_{31}H_{33}N_2^+$: 432.2643.

2.2.7 Bis(dipyrrinato)zinc(II) Complex $2c_2Zn$

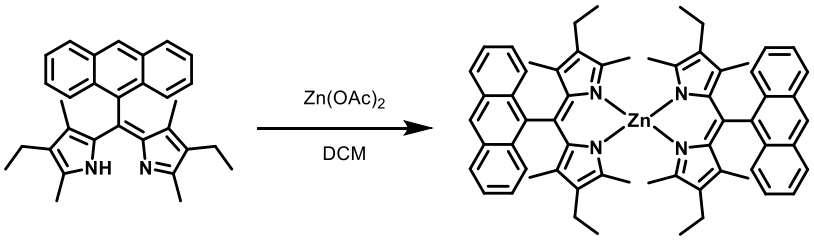

2cH **$2c_2Zn$**

To a dichloromethane solution (10 mL) of **2cH** (0.18 g, 0.50 mmol), was added a methanol (20 mL) solution of zinc acetate (48 mg, 0.26 mmol). After stirring overnight, the amount of the solvent was reduced by a rotary evaporator. The brown precipitate was collected and rinsed thoroughly with methanol. Yield: 0.191 g (82%), orange powder. ^{1}H NMR (500 MHz, $CDCl_3$): δ = 8.59 (s, 2H), 8.09 (d, J = 8.5 Hz, 4H), 8.06 (d, J = 8.5 Hz, 4H), 7.51-7.48 (m, 4H), 7.43-7.40 (m, 4H), 2.29 (s, 12H), 2.19 (d, J = 7.6 Hz, 8H), 0.87 (d, J = 7.6 Hz, 12H), 0.39 (s, 12H); ^{13}C NMR (125 MHz, $CDCl_3$): δ =155.62, 139.14, 137.96, 136.28, 135.28, 131.65, 131.33, 131.24, 128.04, 126.91, 126.16, 125.99, 125.28, 17.88, 15.06, 14.83, 11.92; HR-ESI-MS: 926.4224 $[M]^+$, calcd. for: $C_{62}H_{62}N_4Zn^+$: 926.4266.

2.2.8 Dipyrrin Ligand 3bH

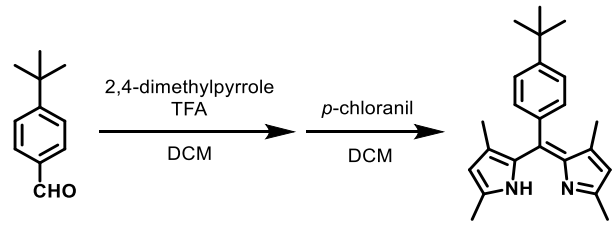

3bH

To a dichloromethane solution (100 mL) of 4-*tert*-butylbenzaldehyde (1.7 g, 10 mmol), were added 2,4-dimethylpyrrole (2.2 mL, 22 mmol) and trifluoroacetic acid (25 μL, 0.33 mmol). After stirring

overnight, *p*-chloranil (2.70 g, 11.0 mmol) was added to the solution and stirred for 20 min. The solvent was evaporated and the residue was purified by alumina column chromatography (hexane: dichloromethane = 2:1). Yield: 0.904 g (27 %), brown powder. ^{1}H NMR (500 MHz, $CDCl_3$): δ = 7.41 (d, J = 8.5 Hz, 2H), 7.19 (d, J = 8.5 Hz, 2H), 5.88 (s, 2H), 2.34 (s, 6H), 1.36 (s, 9H), 1.29 (s, 6H) pyrrolic proton signal (1H) missing due to broadening; ^{13}C NMR (125 MHz, $CDCl_3$): δ =151.57, 151.34, 140.50, 139.23, 136.57, 134.92, 128.78, 125.29, 119.41, 34.69, 31.49, 16.04, 14.35; HRFAB-MS: 333.2333 $[M+H]^+$, calcd. for: $C_{23}H_{29}N_2^+$: 333.2330.

2.2.9 Bis(dipyrrinato)zinc(II) Complex 3b$_2$Zn

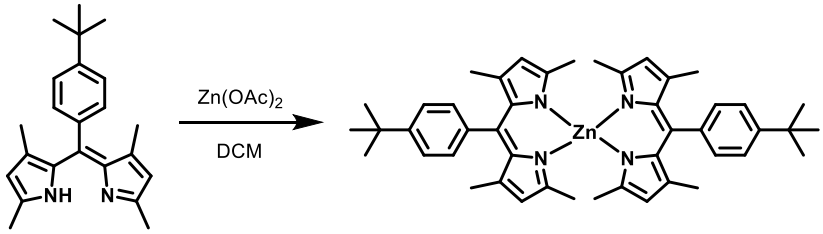

3bH **3b$_2$Zn**

To a dichloromethane solution (10 mL) of **3bH** (0.102 g, 0.306 mmol), was added a methanol (20 mL) solution of zinc acetate (28 mg, 0.15 mmol). After stirring overnight, the amount of the solvent was reduced by a rotary evaporator. The orange precipitate was collected and rinsed thoroughly with methanol. Yield: 0.085 g (78%), orange powder. ^{1}H NMR (500 MHz, $CDCl_3$): δ = 7.44 (d, J = 8.5 Hz, 4H), 7.20 (d, J = 8.5 Hz, 4H), 5.94 (s, 4H), 2.04 (s, 12H), 1.37 (s, 18H), 1.29 (s, 12H); ^{13}C NMR (125 MHz, $CDCl_3$): δ=156.58, 151.41, 145.01, 144.31, 137.01, 135.83, 128.88, 125.31, 120.11, 34.67, 31.53, 16.18, 15.50; HRESI-MS: 1475.7158 $[2M+Na]^+$, calcd. for: $(C_{46}H_{54}N_4Zn)_2Na^+$: 1475.7178.

2.2.10 Dipyrrin Ligand 3cH

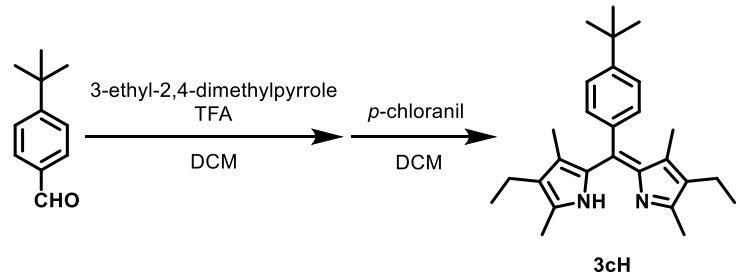

3cH

To a dichloromethane solution (100 mL) of 4-*tert* -butylbenzaldehyde (0.84 mL, 5.0 mmol), were added 3-ethyl-2,4-dimethylpyrrole (1.07 mL, 11.0 mmol) and trifluoroacetic acid (100 μL, 1.30 mmol). After stirring overnight, *p*-chloranil (1.23 g, 5.00 mmol) was added to the solution and stirred for 20 min. The solvent was evaporated and the residue was purified by alumina column chromatography (hexane: dichloromethane = 2:1). Yield: 0.407 g (48 %), brown powder. ^{1}H NMR (500 MHz, $CDCl_3$): δ = 7.40 (d, J = 8.2 Hz, 2H), 7.20 (d, J = 8.2 Hz, 2H), 2.31 (s, 6H), 2.27 (q, J = 7.6 Hz, 4H), 1.35 (s, 9H), 1.19 (s, 6H), 0.87 (t, J = 7.6 Hz, 6H), pyrrolic proton signal (1H) missing due to broadening; ^{13}C NMR (125 MHz, $CDCl_3$): δ=151.32, 149.88, 137.84, 136.16, 135.65, 134.83, 131.11, 129.12, 125.11, 34.64, 31.47, 17.58, 14.86, 14.36, 11.64; HRFAB-MS: 389.2935 $[M]^+$, calcd. for: $C_{27}H_{37}N_2^+$: 389.2957.

2.2.11 Bis(dipyrrinato)zinc(II) Complex 3c$_2$Zn

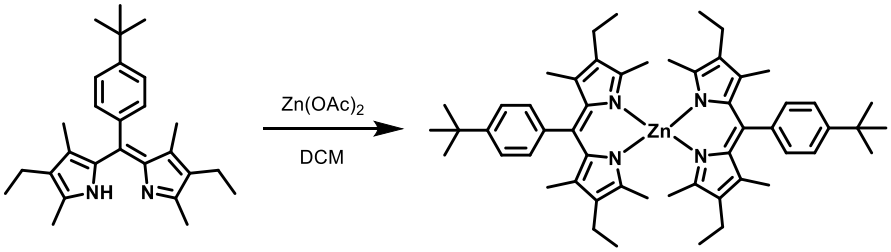

3cH 3c$_2$Zn

To a dichloromethane solution (10 mL) of **3cH** (0.390 g, 1.00 mmol), was added a methanol (20 mL) solution of zinc acetate (0.096 mg, 0.52 mmol). After stirring overnight, the amount of the solvent was reduced by a rotary evaporator. The orange precipitate was collected and rinsed thoroughly with methanol. Yield: 0.401 g (95%), orange powder. ^{1}H NMR (500 MHz, $CDCl_3$): δ = 7.43 (d, J = 8.5

Hz, 4H), 7.23 (d, J = 8.5 Hz, 4H), 2.25 (q, J = 7.5 Hz, 8H), 1.96 (s, 12H), 1.39 (s, 18H), 1.19 (s, 12H), 0.92 (t, J = 7.5 Hz, 12H); ^{13}C NMR (125 MHz, $CDCl_3$): δ=155.59, 151.24, 143.80, 138.40, 137.94, 135.61, 131.32, 129.42, 125.14, 34.66, 31.56, 17.90, 15.01, 14.40, 12.67; HRESI-MS: 838.4840 $[M]^+$, calcd. for: $C_{54}H_{70}N_4Zn^+$: 838.4892.

2.2.12 Apparatus

^{1}H NMR and ^{13}C NMR data were collected in $CDCl_3$ on a Bruker DRX 500 spectrometer. Tetramethylsilane (δH = 0.00) was used as an internal standard for the ^{1}H NMR spectra, and $CDCl_3$ (δC = 77.00) was used as an interrnal standard for the ^{13}C NMR spectra, respectively. High resolution mass spectrometry was performed on either of a JEOL JMS-700MStation mass spectrometer (HRFAB-MS) or a Waters LCT Premier XE spectrometer (HRESI-MS). UV-vis absorption spectra were recorded with a JASCO V- 570 spectrometer. Steady-state fluorescence spectra were collected with a HITACHI F-4500 spectrometer. Absolute photo luminescent quantum yields were collected with a Hamamatsu Photonics C9920-02G. Fluorescence lifetime measurements were performed using a Hamamatsu Photonics Quantaurus-Tau C11367-02. Thermogravimetric analysis was performed under a nitrogen atmosphere using Rigaku Thermo Plus2 TG8120. Al_2O_3 was used as a reference compound, and both nanosheet and Al_2O_3 were mounted on an Al pan. The temperature was controlled from r.t. to 500 °C with a scan rate of 10 °C s^{-1}.

2.2.13 Single-crystal X-ray diffraction analysis

Single crystals suitable for X-ray diffraction analysis were obtained by vapor diffusion, for each single crystal, solvents used (good/poor) are: **1a$_2$Zn** (chloroform / methanol); **1c$_2$Zn·MeOH** (dichloromethane / methanol); **2a$_2$Zn·3CH$_2$Cl$_2$** (dichloromethane / ethanol); **2b$_2$Zn·2CH$_2$Cl$_2$** (dichloromethane / n-hexane); **2c$_2$Zn·CH$_2$Cl$_2$** (dichloromethane / methanol); **3b$_2$Zn** (dichloromethane / methanol); and **3c$_2$Zn** (dichloromethane / ethanol). Synchrotron radiation (SR) X-ray diffraction data of **2a$_2$Zn·3CH$_2$Cl$_2$** and **2c2Zn·CH$_2$Cl$_2$** were collected at 100K. The diffractions were recorded on a CCD detector at SPring-8 beam line BL02B1 (Hyogo, Japan) (SR, λ = 0.3540 Å).X-ray diffraction data of **3c$_2$Zn** were collected at 93 K on a Rigaku Saturn724 (Varimax dual) diffractometer with multi-layer mirror monochromated MoKα radiation (λ = 0.71075 Å). X-ray diffraction data of **1a$_2$Zn**, **1c$_2$Zn·MeOH**, **2b$_2$Zn·2CH$_2$Cl$_2$**, and **3b$_2$Zn** were collected at 113 K with an AFC10 diffractometer coupled with a Rigaku Saturn CCD system equipped with a rotating-anode X-ray generator producing graphite-monochromated MoKα radiation (λ = 0.7107 Å). The structures were solved by direct methods using SIR-92 program (**1a$_2$Zn**, **2b$_2$Zn·2CH$_2$Cl$_2$**), SIR-2004 program (**2a$_2$Zn·3CH$_2$Cl$_2$**, **2c$_2$Zn·CH$_2$Cl$_2$**) or SHELXS97 (**3b$_2$Zn**) and were refined by the full-matrix least-squares techniques against F^2 implementing SHELXL-2013. The structure of **3c$_2$Zn** was solved by the direct method using SIR-2004 program and refined against F^2 using SHELXL-97 Crystallographic data for the structure of **1c$_2$Zn** – **3c$_2$Zn** have been deposited with the Cambridge Crystallographic Data Centre as supplementary publication nos. CCDC 1438041, 1438430, 1438431, 1438015, 1438024, 1438038 and 1438025.

2.3 Molecular design and synthesis

Here, I prepared seven bis(dipyrrinato)zinc(II) complexes to investigate their photophysical properties, which had not been reported to date. As described in Section 2.1, the solid-state luminescence of BODIPYs bearing bulky functional groups can be enhanced because their crystal packing structures are affected by the bulky functional groups. In this context, I designed several dipyrrin ligands bearing a bulky substituent at the *meso*-position of the dipyrrin core, so that the packing structure of the resultant bis(dipyrrinato)zinc(II) complexes would be affected, showing different fluorescence properties.

Here, I have designed a series of dipyrrinato ligands with either of a mesityl, 9-anthracenyl, or 4-*tert*-butylphenyl group on the *meso*-position of the dipyrrin core as the bulky peripheral group. Since alkyl groups affect the electronic structure of the dipyrrin core, dipyrrins with different alkyl substituents were synthesized (Scheme 2.2.1).

The seven dipyrrin ligands **1aH** – **3cH** were prepared through the condensation of an aldehyde and a pyrrole under trifluoracetic acid (TFA) as the acid catalyst, followed by oxidation using *p*-chloranil. The obtained ligands were reacted with zinc acetate to obtain complexes **1a$_2$Zn** – **3c$_2$Zn**.

2.4 Single-crystal X-ray diffraction analysis

Crystal structures and their numerical data are summarized in Figures 2.4.1 – 2.4.7 and Table 2.4.1 – 2.4.7, respectively. In general, the *meso*-aryl group and the dipyrrin core of the complexes in the crystal structure are orthogonal to each other, resulting in minimal electronic interactions of the two subunits. In Figures 2.4.1 and 2.4.3 – 2.4.7, the closest distance of the dipyrrin – dipyrrin planes are depicted (There is no parallel dipyrrin planes showing a distance < 5 Å in **1c・MeOH**). **1a**, **2a・3CH$_2$Cl$_2$**, **2b・2CH$_2$Cl$_2$**, and **2c・CH$_2$Cl$_2$** show closest dipyrrin – dipyrrin distances of 3.321, 3.191, 3.754, and 3.512 Å, respectively. On the other hand, the distances in **3b** and **3c** are 4.601 and 4.433 Å, respectively, significantly larger than those in the rest of the complexes. The difference in the distance arises because of different π-π and CH-π interaction modes between the *meso*-aryl group and the dipyrrin plane. For example, in **2a・3CH$_2$Cl$_2$**, the 9-anthracenyl groups affords CH-π interactions between the anthracene plane and one of C-H bonds on the 9-anthracenyl group, two molecules can come close together, resulting in the small dipyrrin – dipyrrin distance. On the other hand, 4-*tert*-butylphenyl groups cannot accept such interactions, serving as simple bulky functional groups, setting two dipyrrin planes apart. Since π-π interactions are effective when the distance of the two planes are below 4 Å[17,18], **1a**, **2a・3CH$_2$Cl$_2$**, **2b・2CH$_2$Cl$_2$**, and **2c・CH$_2$Cl$_2$** are expected to show effective interactions, while **3b** and **3c** show weaker interactions between the dipyrrin planes. The photophysical properties of the complexes in the solid state are discussed in detail in Section 2.5.

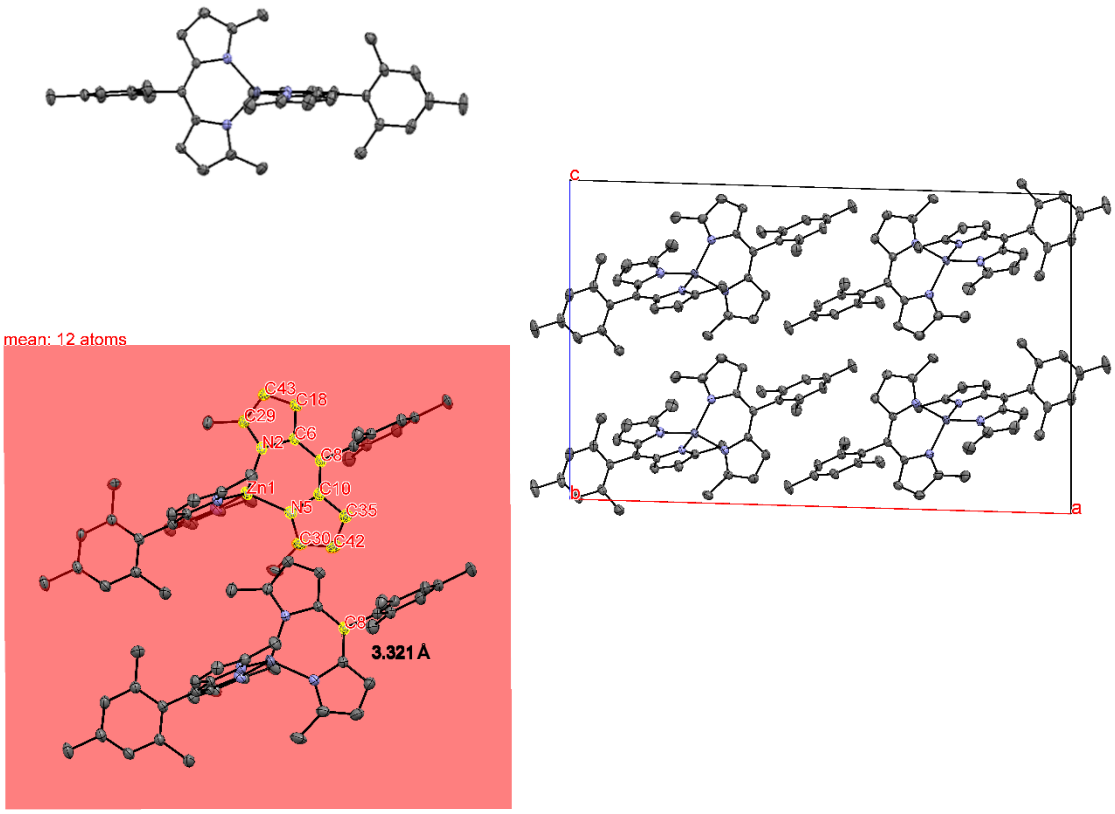

Figure 2.4.1. Crystal structure (top) and packing structures (middle and bottom) of **1a$_2$Zn** (thermal ellipsoids set at 50% probability). Hydrogen atoms and solvent molecules are omitted for clarity. C: gray, N: purple, Zn: dark purple.

Table 2.4.1. Selected crystallographic data of **1a$_2$Zn**

Empirical formula	$C_{40}H_{42}N_4Zn$	V / Å^3	3407.5(8)
Fw / g mol^{-1}	644.15	Z	4
Crystal system	monoclinic	D_{calcd} g/cm^{-3}	1.256
Space group	$P2_1/c$	λ / Å	0.71070
Crystal size / mm	0.6× 0.5 × 0.2	μ / mm^{-1}	0.754
Temperature / K	113	Reflections collected	22668
a / Å	25.853(4)	Independent reflections	7562
b / Å	8.0214(11)	Parameters	406
c / Å	16.439(3)	R_{int}	0.0297
α / º	90	R_1 (I>2.00σ (I)) [a]	0.0409
β / º	91.6890(10)	wR_2 (All reflections) [b]	0.1166
γ / º	90	GoF [c]	1.057

[a]$R_1 = \Sigma||Fo| - |Fc||/\Sigma|Fo|$ ($I > 2\ \sigma(I)$). [b]$wR_2 = [\Sigma(w(Fo^2 - Fc^2)^2/\Sigma w(Fo^2)^2]^{1/2}$ ($I > 2\ \sigma(I)$). [c]GOF = $[\Sigma(w(Fo^2 - Fc^2)^2/\Sigma(Nr - Np)^2]$

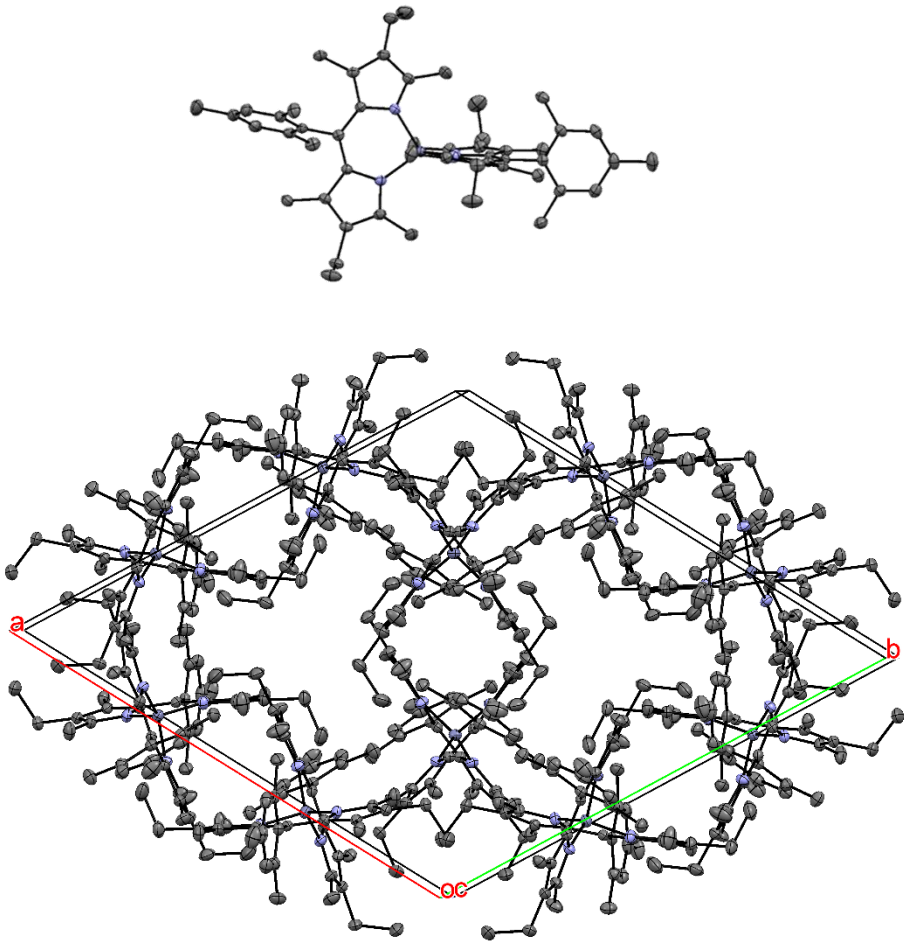

Figure 2.4.2. Crystal structure (top) and packing structure (bottom) of **1c$_2$Zn・MeOH** (thermal ellipsoids set at 50% probability). Hydrogen atoms and solvent molecules are omitted for clarity. C: gray, N: purple,

Table 2.4.2. Selected crystallographic data of **1c$_2$Zn·MeOH**

Empirical formula	$C_{53}H_{69}N_4OZn$	V / Å^3	7227.7(4)
Fw / g mol^{-1}	840.51	Z	6
Crystal system	trigonal	D_{calcd} g/cm^{-3}	1.159
Space group	P-3c1	λ/ Å	0.71070
Crystal size / mm	0.8 × 0.4 × 0.3	μ/ mm^{-1}	0.550
Temperature / K	113	Reflections collected	53931
a / Å	18.4026(4)	Independent reflections	5500
b / Å	18.4026(4)	Parameters	285
c / Å	24.6441(9)	R_{int}	0.0372
α / º	90	R_1 (I>2.00σ (I)) [a]	0.0448
β / º	90	wR_2 (All reflections) [b]	0.1272
γ / º	120	GoF [c]	1.080

[a]$R_1 = \Sigma||Fo| - |Fc||/\Sigma|Fo|$ ($I > 2\ \sigma(I)$). [b]$wR_2 = [\Sigma(w(Fo^2 - Fc^2)^2/\Sigma w(Fo^2)^2]^{1/2}$ ($I > 2\ \sigma(I)$). [c]GOF = $[\Sigma(w(Fo^2 - Fc^2)^2/\Sigma(Nr - Np)^2]$

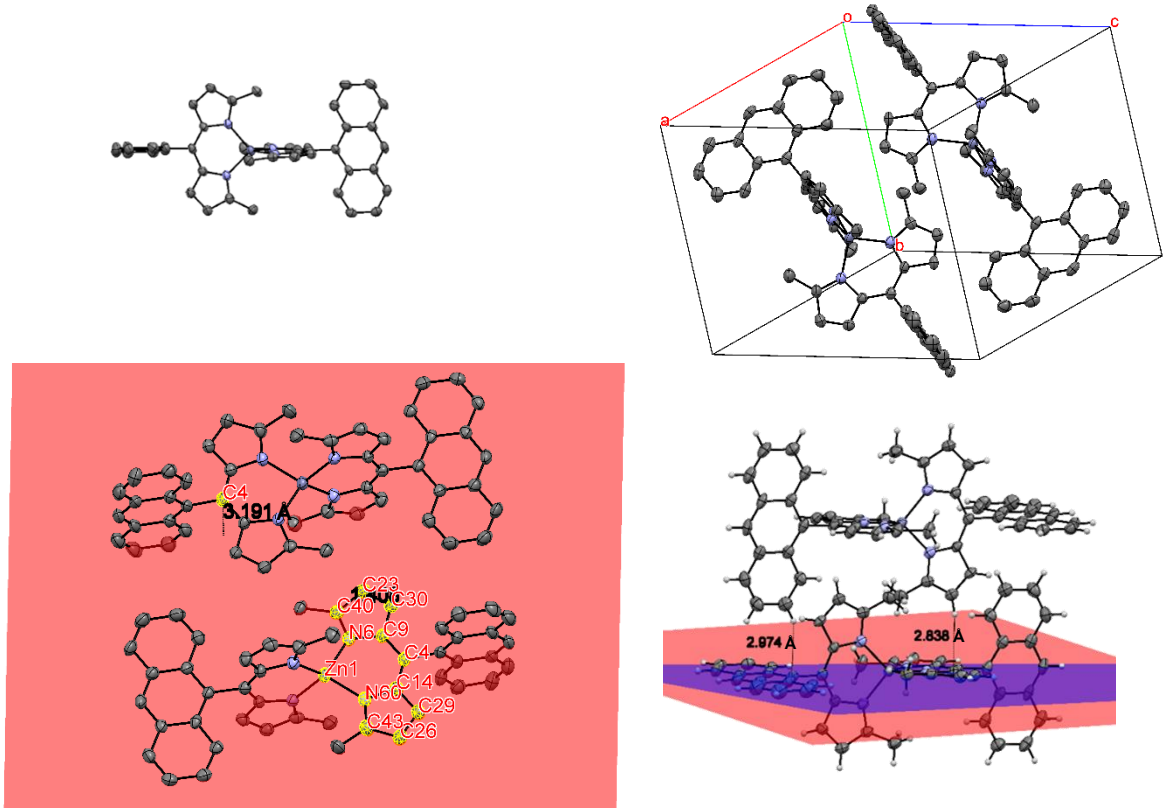

Figure 2.4.3. Crystal structure (top left) and packing structures (top right and bottom) of **2a$_2$Zn** • **3CH$_2$Cl$_2$** (thermal ellipsoids Hydrogen atoms and solvent molecules are omitted for clarity. set at 50% probability). CH-π interactions in the complexes are also displayed (bottom right, blue plane: dipyrrin, red plane: anthracene) C: gray, N: purple, Zn: dark purple.

Table 2.4.3. Selected crystallographic data of **2a$_2$Zn·3CH$_2$Cl$_2$**

Empirical formula	$C_{53}H_{44}Cl_6N_4Zn$	V / Å^3	2323.6(7)
Fw / g mol^{-1}	1015.07	Z	2
Crystal system	triclinic	D_{calcd} g/cm^{-3}	1.351
Space group	P-1	λ / Å	0.35400
Crystal size / mm	0.9 × 0.8 × 0.2	μ/ mm^{-1}	0.137
Temperature / K	100	Reflections collected	40527
a / Å	11.3092(16)	Independent reflections	10655
b / Å	13.973(2)	Parameters	577
c / Å	16.046(3)	R_{int}	0.0981
α / º	102.672(8)	R_1 (I>2.00σ (I)) [a]	0.1136
β / º	107.805(8)	wR_2 (All reflections) [b]	0.3625
γ / º	94.872(7)	GoF [c]	1.294

[a]$R_1 = \Sigma||Fo| - |Fc||/\Sigma|Fo|$ ($I > 2\ \sigma(I)$). [b]$wR_2 = [\Sigma(w(Fo^2 - Fc^2)^2/\Sigma w(Fo^2)^2]^{1/2}$ ($I > 2\ \sigma(I)$). [c]GOF = $[\Sigma(w(Fo^2 - Fc^2)^2/\Sigma(Nr - Np)^2]$

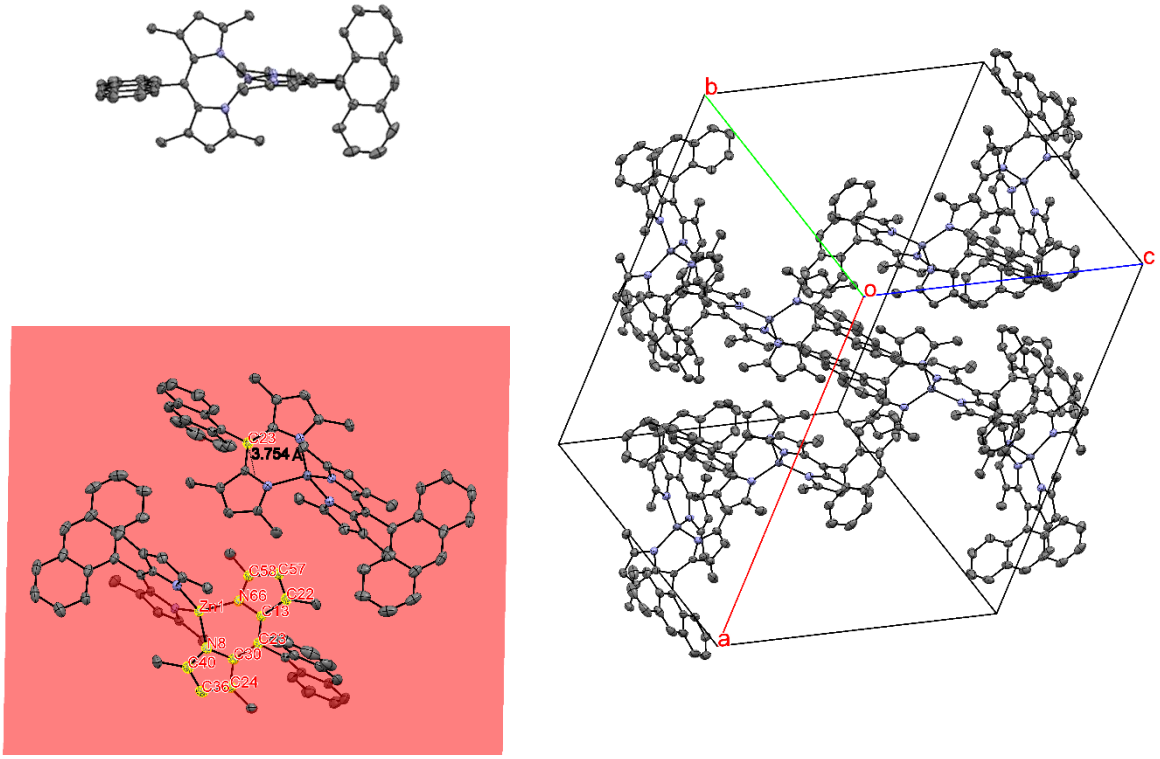

Figure 2.4.4. Crystal structure (top) and packing structures (middle and bottom) of **2b$_2$Zn・2CH$_2$Cl$_2$** (thermal ellipsoids set at 50% probability). Hydrogen atoms and solvent molecules are omitted for clarity. C: gray, N: purple, Zn: dark purple.

Table 2.4.4. Selected crystallographic data of **2b$_2$Zn·2CH$_2$Cl$_2$**

Empirical formula	$C_{56}H_{50}Cl_4N_4Zn$	V / Å^3	9653(7)
Fw / g mol^{-1}	988.25	Z	8
Crystal system	monoclinic	D_{calcd} g/cm^{-3}	1.360
Space group	$C2/c$	λ / Å	0.71070
Crystal size / mm	0.2 × 0.2 × 0.05	μ/ mm^{-1}	0.773
Temperature / K	113	Reflections collected	37213
a / Å	25.180(10)	Independent reflections	11011
b / Å	20.397(8)	Parameters	586
c / Å	18.983(7)	R_{int}	0.0594
α / º	90	R_1 (I>2.00σ (I)) [a]	0.0696
β / º	98.106(5)	wR_2 (All reflections) [b]	0.2237
γ / º	90	GoF [c]	1.039

[a]$R_1 = \Sigma||Fo| - |Fc||/\Sigma|Fo|$ ($I > 2\ \sigma(I)$). [b]$wR_2 = [\Sigma(w(Fo^2 - Fc^2)^2/\Sigma w(Fo^2)^2]^{1/2}$ ($I > 2\ \sigma(I)$). [c]GOF = $[\Sigma(w(Fo^2 - Fc^2)^2/\Sigma(Nr - Np)^2]$

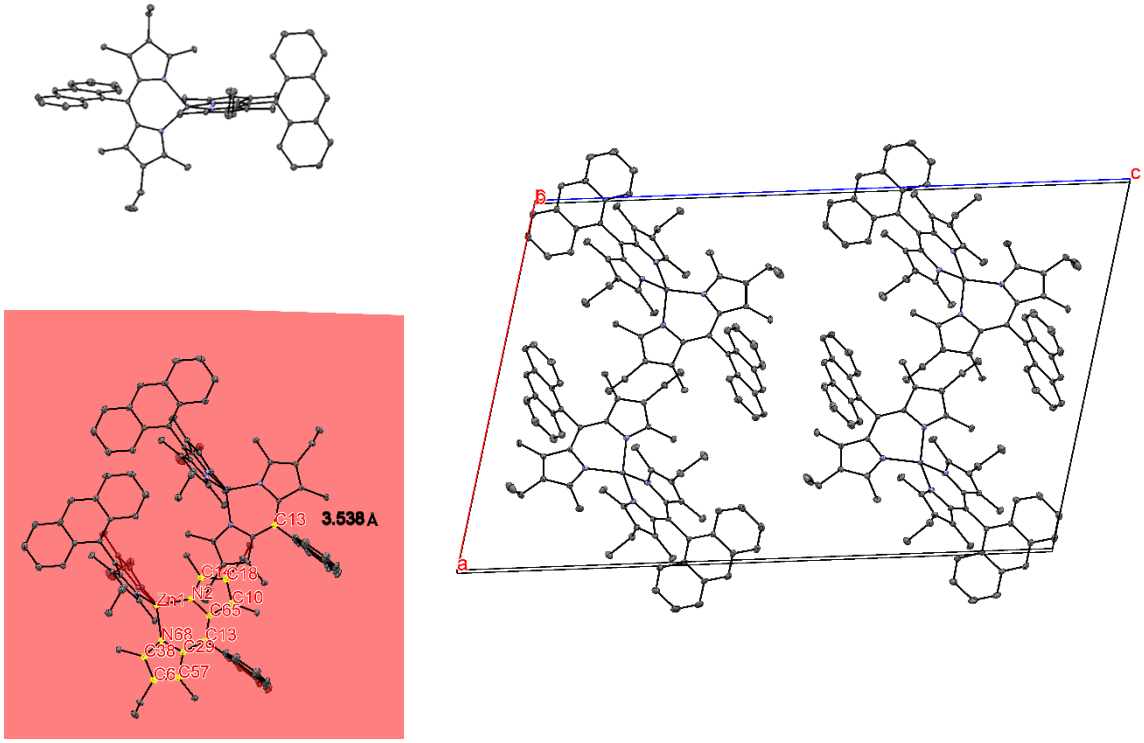

Figure 2.4.5. Crystal structure (top) and packing structures (middle and bottom) of **2c$_2$Zn · CH$_2$Cl$_2$** (thermal ellipsoids set at 50% probability). Hydrogen atoms and solvent molecules are omitted for clarity. C: gray, N: purple, Zn: dark purple.

Table 2.4.5. Selected crystallographic data of **2c$_2$Zn· CH$_2$Cl$_2$**

Empirical formula	$C_{63}H_{64}Cl_2N_4Zn$	V / Å^3	5066.3(3)
Fw / g mol^{-1}	1013.51	Z	4
Crystal system	monoclinic	D_{calcd} g/cm^{-3}	1.329
Space group	$P2_1/c$	λ / Å	0.35400
Crystal size / mm	0.210 × 0.100 × 0.037	μ/ mm^{-1}	0.119
Temperature / K	100	Reflections collected	70431
a / Å	19.6231(4)	Independent reflections	19310
b / Å	8.60965(16)	Parameters	683
c / Å	30.9024(6)	R_{int}	0.0617
α / º	90	R_1 (I>2.00σ (I)) [a]	0.0407
β / º	103.976(8)	wR_2 (All reflections) [b]	0.1092
γ / º	90	GoF [c]	1.056

[a]$R_1 = \Sigma||Fo| - |Fc||/\Sigma|Fo|$ ($I > 2\ \sigma(I)$). [b]$wR_2 = [\Sigma(w(Fo^2 - Fc^2)^2/\Sigma w(Fo^2)^2]^{1/2}$ ($I > 2\ \sigma(I)$). [c]GOF = $[\Sigma(w(Fo^2 - Fc^2)^2/\Sigma(Nr - Np)^2]$

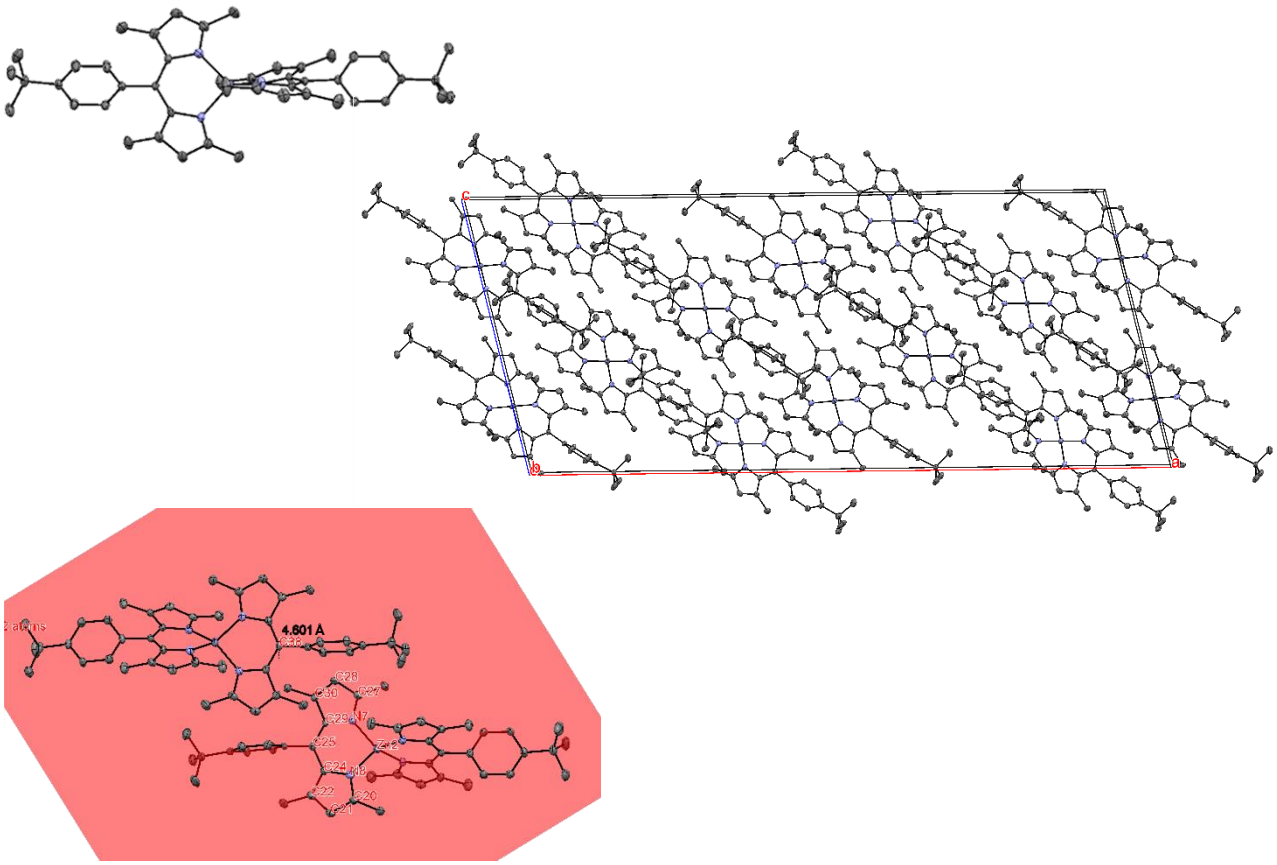

Figure 2.4.6. Crystal structure (top) and packing structures (middle and bottom) of **3b$_2$Zn** (thermal ellipsoids set at 50% probability). Hydrogen atoms and solvent molecules are omitted for clarity. C: gray, N: purple, Zn: dark purple.

Table 2.4.6. Selected crystallographic data of **3b$_2$Zn**

Empirical formula	$C_{46}H_{54}N_4Zn$	V / Å^3	11704(7)
Fw / g mol^{-1}	728.34	Z	12
Crystal system	monoclinic	D_{calcd} g/cm^{-3}	1.240
Space group	$C2/c$	λ / Å	0.71070
Crystal size / mm	0.8 × 0.3 × 0.1	μ/ mm^{-1}	0.667
Temperature / K	113	Reflections collected	36454
a / Å	48.682(15)	Independent reflections	10137
b / Å	11.495(4)	Parameters	690
c / Å	21.478(7)	R_{int}	0.0649
α / º	90	R_1 (I>2.00σ (I)) [a]	0.0737
β / º	103.158(5)	wR_2 (All reflections) [b]	0.1863
γ / º	90	GoF [c]	1.095

[a]$R_1 = \Sigma||Fo| - |Fc||/\Sigma|Fo|$ ($I > 2\ \sigma(I)$). [b]$wR_2 = [\Sigma(w(Fo^2 - Fc^2)^2/\Sigma w(Fo^2)^2]^{1/2}$ ($I > 2\ \sigma(I)$). [c]GOF = $[\Sigma(w(Fo^2 - Fc^2)^2/\Sigma(Nr - Np)^2]$

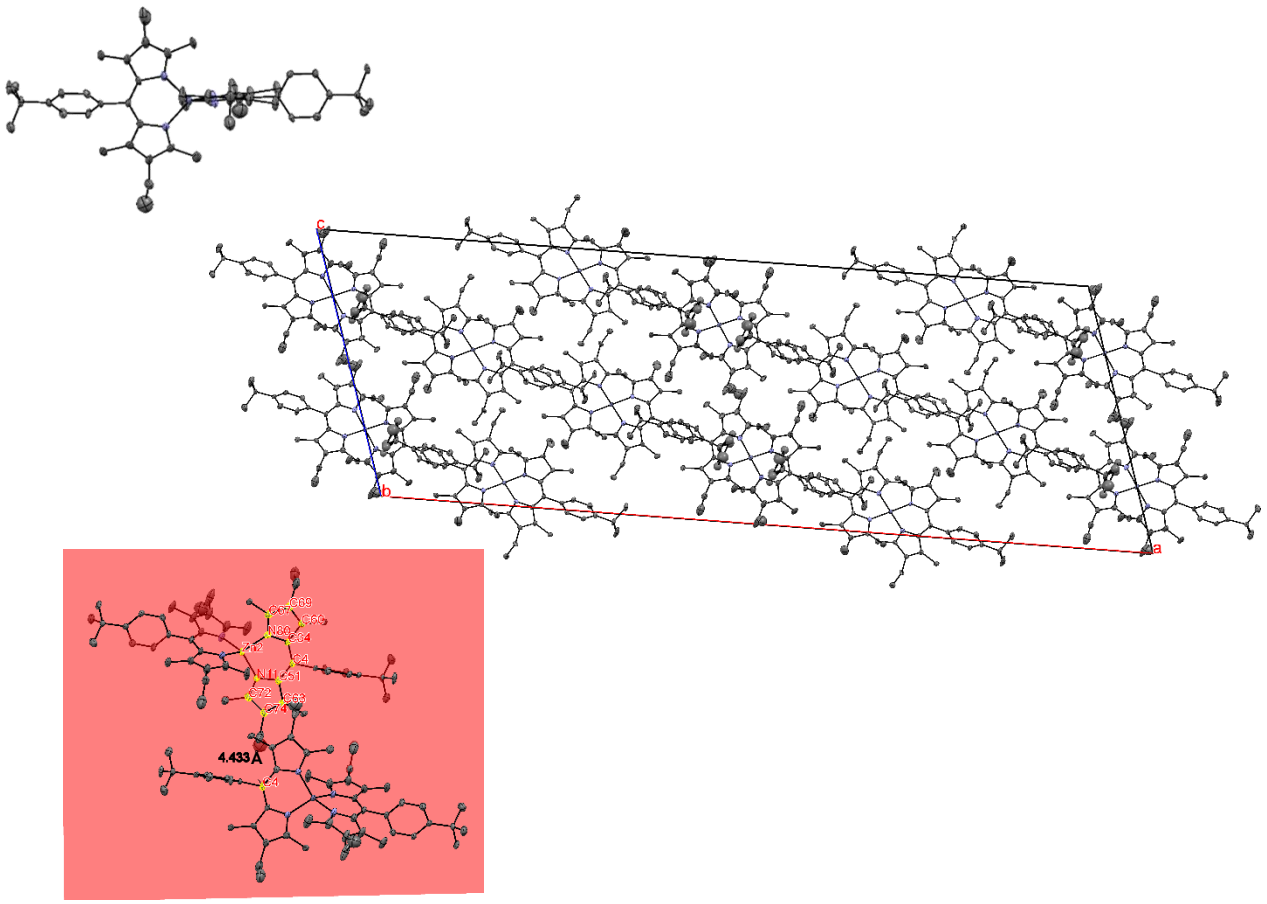

Figure 2.4.7. Crystal structure (top) and packing structures (middle and bottom) of **3c$_2$Zn** (thermal ellipsoids set at 50% probability). Hydrogen atoms and solvent molecules are omitted for clarity. C: gray, N: purple, Zn: dark purple.

Table 2.4.7. Selected crystallographic data of **3c$_2$Zn**

Empirical formula	$C_{54}H_{70}N_4Zn$	V / Å^3	14138(9)
Fw / g mol^{-1}	840.55	Z	12
Crystal system	monoclinic	D_{calcd} g/cm^{-3}	1.185
Space group	$C2/c$	λ / Å	0.71075
Crystal size / mm	0.240 × 0.160 × 0.090	μ/ mm^{-1}	0.561
Temperature / K	93	Reflections collected	40373
a / Å	61.25(2)	Independent reflections	13159
b / Å	11.159(4)	Parameters	795
c / Å	21.726(8)	R_{int}	0.0946
α / º	90	R_1 (I>2.00σ (I)) [a]	0.1000
β / º	107.814(5)	wR_2 (All reflections) [b]	0.2287
γ / º	90	GoF [c]	1.100

[a]$R_1 = \Sigma||Fo| - |Fc||/\Sigma|Fo|$ ($I > 2\ \sigma(I)$). [b]$wR_2 = [\Sigma(w(Fo^2 - Fc^2)^2/\Sigma w(Fo^2)^2]^{1/2}$ ($I > 2\ \sigma(I)$). [c]GOF = $[\Sigma(w(Fo^2 - Fc^2)^2/\Sigma(Nr - Np)^2]$

2.5 Photophysical properties

2.5.1 Spectroscopic properties in toluene solution

The appearance of **1a$_2$Zn** – **3c$_2$Zn** in toluene solution are shown in Figure 2.5.1.1. Photophysical properties of **1a$_2$Zn** – **3c$_2$Zn** in toluene solution are summarized Table 2.5.1.1. Their absorption spectra are depicted in Figure 2.5.1.2. The complexes show absorption maxima in the range of 488 – 511 nm, whose molar extinction coefficients, ε, are 1.21 to 1.6 $\times 10^5$ M^{-1} cm^{-1}. The values are in the typical range of bis(dipyrrinato)zinc(II) complexes, which originate in their $^1\pi$-π^* transition[13]. **2a$_2$Zn** – **2c$_2$Zn** exhibit an additional absorption band centered at approximately 370 nm with vibronic structures, attributed to the $^1\pi$-π^* transition of the 9-anthracenyl unit.[14]

Emission spectra of the complexes are depicted in Figure 2.5.1.3. The emission maxima of the complexes are in the range of 510 – 558 nm, corresponding to the emission of the $^1\pi$-π^* excited state. The complexes bearing 2,6-diethyl groups on the dipyrrin cores of the ligands (**1c$_2$Zn**, **2c$_2$Zn**, and **3c$_2$Zn**) show slightly red-shifted emission maxima compared to the rest of the complexes, presumably due to elevated HOMO levels by the electron-donating alkyl groups, reported in analogous structures[13]. The fluorescence quantum yields of the complexes in solution are below 0.20, four of them showing below 0.01; this can be attributed to the symmetry-breaking charge transfer process between the two identical dipyrrinato ligands, often observed in bichromophoric systems including homoleptic bis(dipyrrinato)zinc(II) complexes reported[10,13,19,20]. The fluorescence lifetimes obtained for the complexes are 2.4 – 4.5 ns, which are in the typical range for similar structures, corresponding to the $^1\pi$-π^* transition[10,14]. Their fluorescence decay is monoexponential, suggesting their fluorescence solely from the $^1\pi$-π^* excited state without any additional photophysical processes.

Overall, there is little difference in their photophysical properties upon the structural difference; the alky groups on the dipyrrin core and the aryl group on the *meso*-position only perturb the electronic structure of the dipyrrin core slightly.

Figure 2.5.1.1. Complexes **1a$_2$Zn** – **3c$_2$Zn** under ambient light (top) and 365 nm irradiation (bottom).

Table 2.5.1.1. Spectroscopic properties of complexes **1a$_2$Zn** – **3c$_2$Zn** in toluene

	λ_{abs}[a] / nm	ε[b] / M^{-1} cm^{-1}	λ_{em} (λ_{ex})[c] / nm	ϕ_F[d]	τ[e] / ns	k_F[f] / s^{-1}	k_{NR}[g] / s^{-1}
1a$_2$Zn	495[h]	1.6[h]	507 (495)[h]	0.28[h]	4.5	6.2×10^7	1.6×10^8
1c$_2$Zn	508[h]	1.4[h]	532 (508)[h]	0.20[h]	2.4	8.3×10^7	3.3×10^8
2a$_2$Zn	498	1.39	513 (484)	0.090	2.8	3.2×10^7	3.3×10^8
2b$_2$Zn	493	1.45	519 (480)	< 0.05	-	-	-
2c$_2$Zn	511	1.29	558 (496)	< 0.01	-	-	-
3b$_2$Zn	488	1.39	510 (470)	< 0.05	4.5	-	-
3c$_2$Zn	506	1.21	538 (490)	< 0.05	-	-	-

[a]absorption maximum [b]molar absorptivity [c]emission maximum (λ_{em}) and excitation wavelength (λ_{ex}) [d]fluorescence quantum yield [e]fluorescence lifetime fitted from fluorescence decay curve [f]radiative decay constant, $k_F = \phi_F/\tau$ [g]non-radiative decay constant, $k_{NR} = (1 - \phi_F)/\tau$ [h]from ref. 13

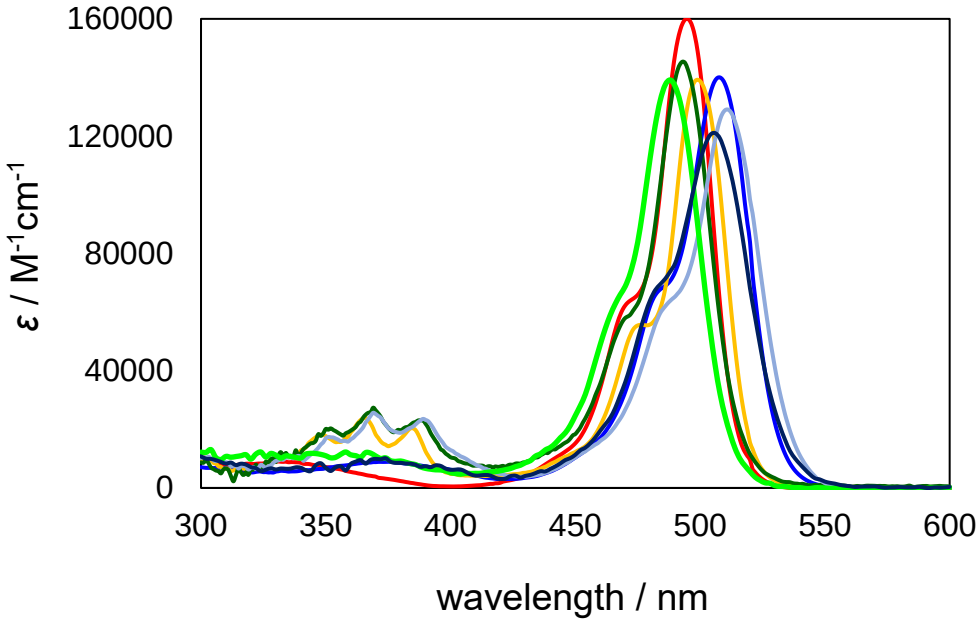

Figure 2.5.1.2. Absorption spectra of complexes **1a$_2$Zn** (red)**, 1c$_2$Zn** (blue)**, 2a$_2$Zn** (orange)**, 2b$_2$Zn** (green)**, 2c$_2$Zn** (light blue)**, 3b$_2$Zn** (pale green)**,** and **3c$_2$Zn** (dark blue) in toluene.

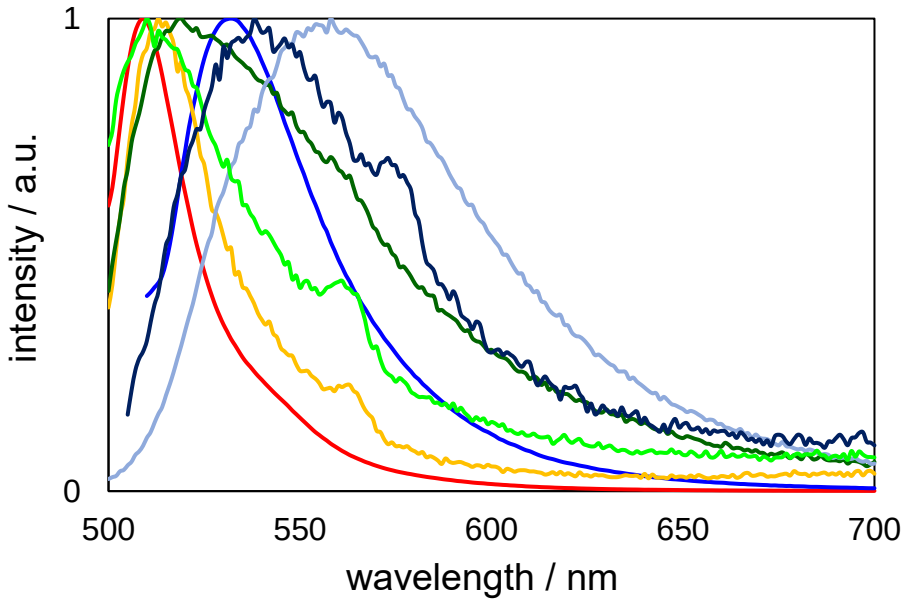

Figure 2.5.1.3. Emission spectra of complexes **1a$_2$Zn** (red)**, 1c$_2$Zn** (blue)**, 2a$_2$Zn** (orange)**, 2b$_2$Zn** (green)**, 2c$_2$Zn** (light blue)**, 3b$_2$Zn** (pale green)**,** and **3c$_2$Zn** (dark blue) in toluene.

2.5.2 Spectroscopic properties in the aggregate and solid state

In sharp contrast to the spectroscopic properties in solution, those in the solid state are remarkably different. Their appearance under ambient light and 365 nm irradiation is shown in Figure 2.5.2.1. Spectroscopic properties of the complexes in the solid state are summarized in Table 2.5.2.1.

Absorption spectra of the complexes as drop cast films are shown in Figure 2.5.2.2. The spectra show 15 – 30 nm red-shifts compared to those in solution, presumably due to stronger intermolecular interactions between the molecules in the aggregate state. Emission in the solid state is depicted in Figure 2.5.2.3.

Emission of the complexes in the solid state exhibits significantly different spectral shape and emission maxima. For example, **1a$_2$Zn**, the complex with *meso*-mesityl and 1,7-dimethyl groups on the dipyrrin core, emits at 615 nm, 108 nm red-shifted from that in solution (507 nm). **2a$_2$Zn**, bearing the same number of methyl groups at the same positions, with a *meso*-anthracenyl group, shows an emission maximum of 635 nm, which is 122 nm red-shifted from that in solution (513 nm) and 20 nm red-shifted from that of **1a$_2$Zn** in the solid state. **3b$_2$Zn**, a complex with a *meso*-4-*tert*-buylphenyl group and 1,3,5,7-tetramethyl groups on the dipyrrin moieties, shows an emission maximum of 560 nm, only a 47 nm red-shift from that in toluene (510 nm). Since the spectral shape of the emission spectra of the complexes are distorted from that in solution, and different from each other, the *meso*-aryl group seems to play important roles in modifying their emission spectra. Since the molecules in the solid state are tightly packed, it is expected that the intermolecular interactions are far stronger than those in solution. As described in Section 2.4, 9-anthracenyl groups allows intermolecular π-π stacking and CH-π interactions, bringing the distance of the molecules close, while 4-*tert*-butylphenyl groups cannot host such interactions as much as 9-anthracenyl groups, simply functioning as bulky functional groups.

The proximity of the dipyrrin cores in the crystals allows various types of interactions to modify the spectroscopic properties of the complexes. Although quantitative analysis is far

complicated from the data obtained, it is assumed that such interactions include exciton coupling and excimer formation. The former is interactions between the transition dipole moments of chromophores in proximity, creating new transition dipoles with different excitation energies, which can be interpreted as "fusion of adjacent chromophores" (Figure 2.5.2.4). The transition dipole of a dipyrrin core is oriented along its long axis. Thus, for the complexes in the solid state, the transition dipoles are aligned in head-to-tail type orientations, resulting in red-shifted transitions.[21] Excimer formation can also be one of the reasons for the red-shifted spectra. The formation of an excimer between the dipyrrin cores would result in a stabilized system, emitting at longer wavelengths. Since there are multiple possible interaction modes in their aggregate states, the resultant spectra are broadened.

Here, bis(dipyrrinato)zinc(II) complexes are found to be fluorescent in the solid state. The *meso*-aryl group plays important roles in modifying the emission spectra of the complexes, which affects the packing structures in the solid state, thus the dipyrrin – dipyrrin interactions and the resultant emission properties.

Table 2.5.2.1. Spectroscopic properties of complexes **1a$_2$Zn** – **3c$_2$Zn** in the solid state

	λ_{abs}[a] (thin film) / nm	λ_{em} (λ_{ex})[b] (solid) / nm	ϕ_F[c]	$\tau_1(f_1)$, $\tau_2(f_2)$[d] / ns	$\langle\tau\rangle$[e] / ns
1a$_2$Zn	519	615 (500)	0.02	0.64 (65%), 2.0 (35%)	1.2
1c$_2$Zn	530	575 (510)	-	-	-
2a$_2$Zn	528	635 (510)	0.03	0.43 (57%), 1.0 (43%)	0.68
2b$_2$Zn	517	609 (510)	<0.01	-	-
2c$_2$Zn	526	581 (510)	0.01	-	-
3b$_2$Zn	511	560 (470)	0.03	0.37 (98%), 1.7 (2%)	0.50
3c$_2$Zn	521	608 (510)	<0.01	-	-

[a]absorption maximum [b]emission maximum (λ_{em}) and excitation wavelength (λ_{ex}) [c]fluorescence quantum yield [d]fluorescence lifetime fitted from fluorescence decay curve [e]average fluorescence lifetime

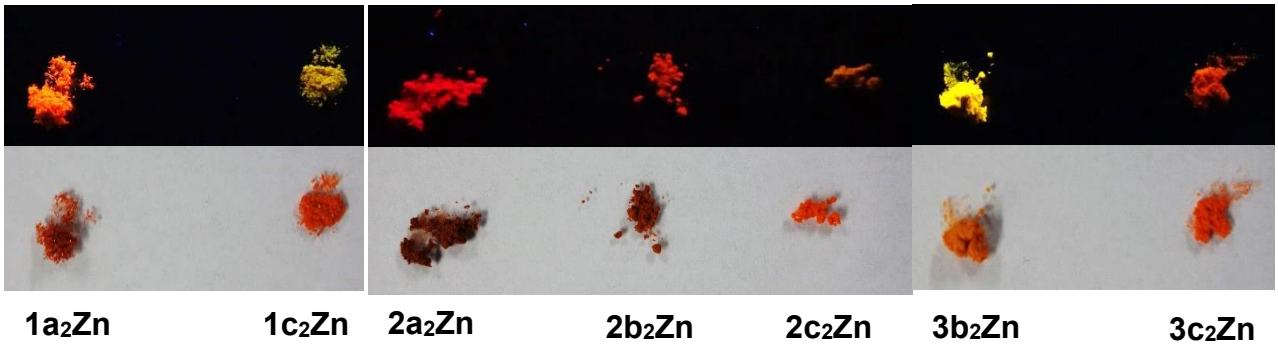

Figure 2.5.2.1. Complexes **1a$_2$Zn** – **3c$_2$Zn** under irradiation at 365 nm (top) and ambient light (bottom).

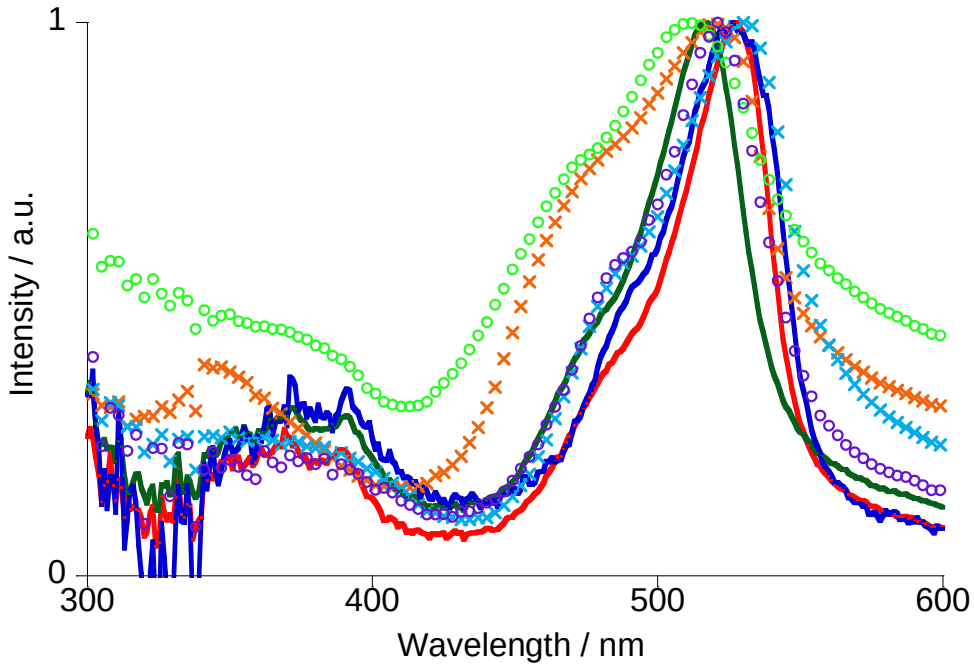

Figure 2.5.2.2. Absorption spectra of complexes **1a$_2$Zn** (orange cross marks), **1c$_2$Zn** (light blue cross marks), **2a$_2$Zn** (red solid line), **2b$_2$Zn** (green solid line), **2c$_2$Zn** (blue solid line), **3b$_2$Zn** (light green open circles), and **3c$_2$Zn** (purple open circles) on quartz substrate.

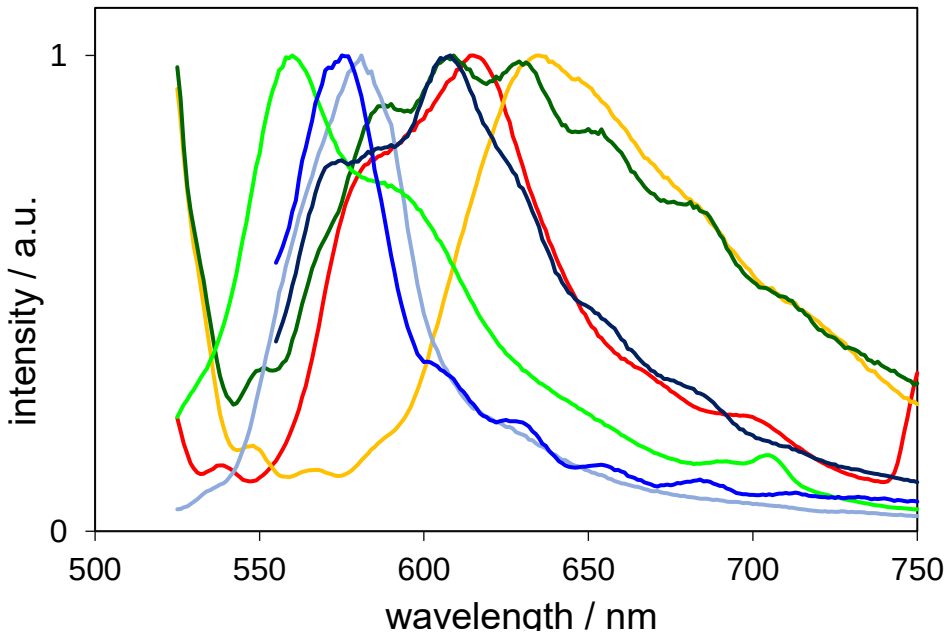

Figure 2.5.2.3. Emission spectra of **1a$_2$Zn** (red), **1c$_2$Zn** (blue), **2a$_2$Zn** (orange), **2b$_2$Zn** (green), **2c$_2$Zn** (light blue), **3b$_2$Zn** (pale green), and **3c$_2$Zn** (dark blue).

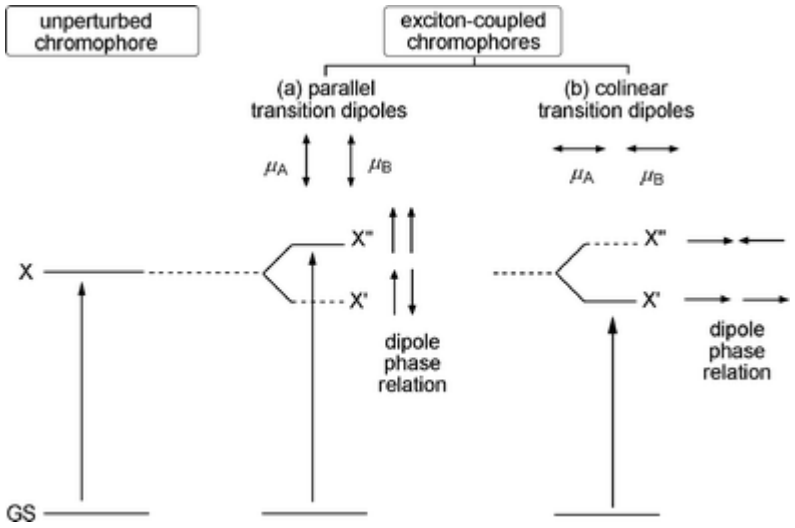

Figure 2.5.2.4 Exciton coupling of two chromophores. Note that in oblique orientations, both the transition to the X' and X'' states are possible.[21] Fluorescence can be interpreted as a transition from X' or X'' to GS, the opposite transition of the depicted ones. Reproduced from ref. 21 with permission from the Royal Society of Chemistry.

2.6 Conclusion

In this chapter, fluorescence properties of bulky-substituent bearing bis(dipyrrinato)zinc(II) complexes have been revealed. Their spectroscopic properties in solution, drop-cast film, and the solid-state have been obtained, showing distinctly different spectral shape, absorption and emission maxima, and fluorescence lifetimes. Single-crystal X-ray diffractional analysis was performed and their crystal structures were obtained. Each crystal structure shows unique packing structure, resulting in different spectroscopic properties in the solid state. Through this study, bis(dipyrrinato)zinc(II) complexes were found to be fluorescent and the packing structure was found to be important for the luminescence properties.

2.7 References

1. Aratani, N.; Kim, D.; Osuka, A. *Acc. Chem. Res.* **2009**, *42*, 1922–1934.
2. Jeong, Y. H.; Son, M.; Yoon, H.; Kim, P.; Lee, D. H.; Kim, D.; Jang, W. D. *Angew. Chem. Int. Ed.* **2014**, *53*, 6925–6928.
3. Balaban, T. S. *Acc. Chem. Res.* **2005**, *38*, 612–623.
4. Lin, X. H.; Lee, S. N.; Zhang, W.; Li, S. F. Y. *J. Hazard. Mater.* **2016**, *303*, 64–75.
5. Irmler, P.; Winter, R. F. *Dalton Trans.* **2016**, *45*, 10420–10434.
6. Sasabe, H.; Kido, J. *Eur. J. Org. Chem.* **2013**, No. 34, 7653–7663.
7. Sasabe, H.; Kido, J. *J. Mater. Chem. C* **2013**, *1*, 1699–1707.
8. Kido, J.; Kimura, M.; Nagai, K. *Science* **1995**, *267*, 1332–1334.
9. Wood, T. E.; Thompson, A. *Chem. Rev.* **2007**, *107*, 1831–1861.
10. Yu, L.; Muthukumaran, K.; Sazanovich, I. V; Kirmaier, C.; Hindin, E.; Diers, J. R.; Boyle, P. D.; Bocian, D. F.; Holten, D.; Lindsey, J. S. *Inorg. Chem.* **2003**, *42*, 6629–6647.
11. Sakamoto, R.; Iwashima, T.; Tsuchiya, M.; Toyoda, R.; Matsuoka, R.; Kögel, J. F.; Kusaka, S.; Hoshiko, K.; Yagi, T.; Nagayama, T.; Nishihara, H. *J. Mater. Chem. A* **2015**, *3*, 15357–15371.
12. Baudron, S. A. *Dalton Trans.* **2013**, *42*, 7498–7509.
13. Kusaka, S.; Sakamoto, R.; Kitagawa, Y.; Okumura, M.; Nishihara, H. *Chem. Asian J.* **2012**, *7*, 907–910.
14. Tsuchiya, M.; Sakamoto, R.; Kusaka, S.; Kitagawa, Y.; Okumura, M.; Nishihara, H. *Chem. Commun.* **2014**, *50*, 5881–5883.
15. Maeda, H.; Hasegawa, M.; Hashimoto, T.; Kakimoto, T.; Nishio, S.; Nakanishi, T. *J. Am. Chem. Soc.* **2006**, *128*, 10024–10025.
16. Ozdemir, T.; Atilgan, S.; Kutuk, I.; Yildirim, L. T.; Tulek, A.; Bayindir, M.; Akkaya, E. U. *Org. Lett.* **2009**, *11*, 2105–2107.

17. Hunter, C. A.; Sanders, J. K. M. *J. Am. Chem. Soc.* **1990**, *112*, 5525–5534.

18. Janiak, C. *Dalton Trans.* **2000**, *21,* 3885–3896.

19. Trinh, C.; Kirlikovali, K.; Das, S.; Ener, M. E.; Gray, H. B.; Djurovich, P.; Bradforth, S. E.; Thompson, M. E. *J. Phys. Chem. C. Nanomater. Interfaces* **2014**, *118*, 21834–21845.

20. Mataga, N.; Yao, H.; Okada, T.; Rettig, W. *J. Phys. Chem.* **1989**, *93*, 3383–3386.

21. Telfer, S. G.; McLean, T. M.; Waterland, M. R. *Dalton Trans.* **2011**, *40*, 3097–3108.

Chapter 3

Synthesis and Spectroscopic Properties of Imine-linked BODIPYs

第３章
本章については、５年以内に雑誌等で刊行予定のため、非公開。

Chapter 4

Concluding remarks

Throughout this thesis, I focused on the synthesis and photophysics of dipyrrinato metal complexes. I have developed and evaluated the newly synthesized dipyrrinato metal complexes, which were found to be luminescent under "assembled" states.

In Chapter 1, I described the importance of photofunctional molecules and their applications. I also portrayed dipyrrins and dipyrrinato metal complexes, whose chemical and photochemical properties are favorable in constructing photofunctional molecules.

In Chapter 2, I developed a series of bis(dipyrrinato)zinc(II) complexes bearing bulky *meso*-aryl groups. The complexes were revealed to be luminescent in the solid state, whose emission was concluded to be dependent on the packing structure, especially the dipyrrin – dipyrrin distances. Exciton coupling and excimer formation are two possible interactions for the complexes in the solid state. In this chapter, bis(dipyrrinato)zinc(II) complexes were demonstrated to be fluorescent in the solid state.

In Chapter 3, I designed several types of imine-linked BODIPYs. Formyl group(s) were appended on the 2- and 6- positions of the BODIPY core, and several types of amine were reacted to the BODIPYs. The reaction proceeded quickly under mild conditions, such as room temperature and ambient atmosphere. The photophysical properties of the complexes were found to be dependent on the type of the linkage. For example, the alkylimine-bridged ones showed relatively unmodified photophysical properties, while the hydrazone-bridged ones showed π-extension through the hydrazone bridge. The imine-linked BODIPYs, both the alkylimine-bridged ones and hydrazone-bridged ones are found to be fluorescent, in moderate to high fluorescence quantum yields, showing applicability as fluorophores. BODIPYs were also immobilized onto amino-terminated silica gel. The reaction also proceeded quickly and the BODIPY-supported silica gel was intensely fluorescent. The synthetic convenience of the imine linkage and compatibility with BODIPYs in terms of fluorescence were illustrated through this chapter.

To conclude my thesis, a series of dipyrrinato metal complexes and their assemblies were developed and synthesized. Their synthesis and molecular design were carefully devised under the concept of distance and orientation of the resultant assembled states. The synthesized complexes were demonstrated to be fluorescent in the assembled states. The distance and orientation of the assembled dipyrrin complexes influence the photophysical properties. The projects contribute to the chemistry and photophysics of dipyrrins by providing knowledge and insight of multi-chromophoric systems. The concepts and results in this thesis also lead to development of photofunctional materials with multiple chromophoric units.

Acknowledgement

I would like to show my gratitude to those who supported the accomplishment of my Ph.D. course research.

Professor Dr. Hiroshi Nishihara offered me generous support of helpful advice, the opportunity to conduct experiments. He has provided me with research environments to pursue my Ph.D. course study.

I am deeply grateful to Assistant Professor Dr. Ryota Sakamoto for his beneficial comments and discussion. He has helped me in setting research topics and providing directions to enrich my research.

I would like to express appreciation to Associate Professor Dr. Yoshinori Yamanoi, Assistant Professor Dr. Tetsuro Kusamoto, Project Assistant Professor Dr. Mariko Miyachi, Project Assistant Professor Dr. Wu Kuo Hui, and Project Assistant Professor Dr. Hiroaki Maeda for providing me with suggestions to improve my research.

There are researchers supported my Ph.D. course study technically. I am thankful to Professor Dr. Eiji Nishibori (Graduate School of Pure and Applied Science, University of Tsukuba) and Dr. Kunihisa Sugimoto (Japan Synchrotron Radiation Research Institute) for synchrotron radiation single crystal X-ray diffraction measurements. I would give recognition to Dr. Hideki Waragai (University of Tokyo) for solid-state luminescence measurements.

I am deeply grateful to all Nishiara Laboratory members. I give special thanks to Project Assistant Professor Dr. Shinpei Kusaka (Kyoto University), Dr. Julius F. Kögel, Mr. Toshiki Iwashima, Mr. Ryojun Toyoda, and Mr. Risa Aoki, the members of the dipyrrin group. I also show my gratitude to Dr. Yohei Hattori, Dr. Takamasa Tsukamoto, and Mr. Masaki Shimada for fruitful discussion in crystallography and photochemistry. I am grateful to my colleagues Ms. Yasuyo Ogino, Mr. Ryota Matsuoka, and Mr. Ken Hoshiko for encouraging me during my Ph.D. course.

I am indebted to the JSPS Fellowship for Young Scientists and ALPS program for financial support and providing opportunities to expand my research.

Most of Figures and Tables in Chapter 2 are reproduced from my publication in *Inorganic Chemistry* published in 2016. I also show my gratitude to the American Chemical Society for giving permission to reuse them in this thesis.

Lastly, I show my deepest gratitude to my family for mentally supporting me during my Ph.D. course study.

January 11 2017

Mizuho Tsuchiya

List of publications

【Publication related to the thesis】

1. "Homoleptic Bis(dipyrrinato)zinc(II) Complexes: Emission in the Solid State" Mizuho Tsuchiya, Ryota Sakamoto, Masaki Shimada, Yoshinori Yamanoi, Yohei Hattori, Kunihisa Sugimoto, Eiji Nishibori, Hiroshi Nishihara, *Inorg. Chem.* **2016**, *55*, 5732-5734.

【Publications not related to the thesis】

2. "Dissymmetric Bis(dipyrrinato)zinc(II) Complexes: Rich Variety and Bright Red to Near-Infrared Luminescence with a Large Pseudo-Stokes Shift" Ryota Sakamoto, Toshiki Iwashima, Julius F. Koegel, Shinpei Kusaka, Mizuho Tsuchiya, Yasutaka Kitagawa, Hiroshi Nishihara, *J. Am. Chem. Soc.* **2016**, *138*, 5666-5677.
3. "Bright Solid-state Emission of Disilane-bridged Donor-Acceptor-Donor and Acceptor-Donor-Acceptor Chromophores" Masaki Shimada, Mizuho Tsuchiya, Ryota Sakamoto, Yoshinori Yamanoi, Eiji Nishibori, Kunihisa Sugimoto, Hiroshi Nishihara, *Angew. Chem. Int. Ed.* **2016**, *55*, 3022-3026.
4. "Heteroleptic [Bis(oxazoline)](dipyrrinato)zinc(II) Complexes: Bright and Circularly Polarized Luminescence from an Originally Achiral Dipyrrinato Ligand" Julius F. Koegel, Shinpei Kusaka, Ryota Sakamoto, Toshiki Iwashima, Ryojun Toyoda, Mizuho Tsuchiya, Ryota Matsuoka, Tsukamoto Takamasa, Junpei Yuasa, Yasutaka Kitagawa, Tsuyoshi Kawai, Hiroshi Nishihara, *Angew. Chem. Int. Ed.* **2016**, *55*, 1377-1381.
5. "New aspects in bis and tris(dipyrrinato)metal complexes: bright luminescence, self-assembled nanoarchitectures, and materials applications" Ryota Sakamoto, Toshiki Iwashima, Mizuho Tsuchiya, Ryojun Toyoda, Ryota Matsuoka, Julius F Kogel, Shinpei Kusaka, Ken Hoshiko, Toshiki Yagi, Tatsuhiro Nagayama, Hiroshi Nishihara, *J. Mater. Chem. A* **2015**, *3*, 15357-15371.
6. "Heteroleptic bis(dipyrrinato)copper(II) and nickel(II) complexes" Ryojun Toyoda, Mizuho Tsuchiya, Ryota Sakamoto, Ryota Matsuoka, Kuo-Hui Wu, Yohei Hattori, Hiroshi Nishihara, *Dalton Trans.* **2015**, *44*, 15103-15106.
7. "Bis(dipyrrinato)metal(II) coordination polymers: Crystallization, exfoliation into single wires, and electric conversion ability" Ryota Matsuoka, Ryojun Toyoda, Ryota Sakamoto, Mizuho Tsuchiya, Ken Hoshiko, Tatsuhiro Nagayama, Yoshiyuki Nonoguchi, Kunihisa Sugimoto, Eiji Nishibori, Tsuyoshi Kawai, Hiroshi Nishihara, *Chem. Sci.* **2015**, *6*, 2853-2858.
8. "A photofunctional bottom-up bis(dipyrrinato)zinc(II) complex nanosheet" Ryota Sakamoto, Ken Hoshiko, Qian Liu, Toshiki Yagi, Tatsuhiro Nagayama, Shinpei Kusaka, Mizuho Tsuchiya, Yasutaka Kitagawa, Wai-Yeung Wong, Hiroshi Nishihara, *Nature Commun.* **2015**, *6*, 6713.
9. "New aspects in bis and tris(dipyrrinato)metal complexes: bright luminescence, self-assembled nanoarchitectures, and materials applications" Ryota Sakamoto, Toshiki Iwashima, Tsuchiya Mizuho, Ryojun Toyoda, Ryota Matsuoka, Julius F. Koegel, Shinpei Kusaka, Ken Hoshiko, Toshiki Yagi, Tatsuhiro Nagayama, Hiroshi Nishihara, *J. Mater. Chem. A* **2015**, *3*, 15357-15371.

10. "Acid-Responsive Fluorescent Compounds Based on Nitro-Group-Substituted L-Shaped Pentacycles, Pyrrolo[1,2-*a*][1,8]naphthyridines" Kotaro Tateno, Rie Ogawa, Ryota Sakamoto, Mizuho Tsuchiya, Takashi Otani, Takao Saito, *Org. Lett.* **2014**, *16*, 3212-3215.
11. "Asymmetric dinuclear bis(dipyrrinato)zinc(II) complexes: Broad absorption and unidirectional quantitative exciton transmission" Mizuho Tsuchiya, Ryota Sakamoto, Shinpei Kusaka, Yasutaka Kitagawa, Mitsutaka Okumura, Hiroshi Nishihara, *Chem. Commun.* **2014**, *50*, 5881-5883.